Available online at www.sciencedirect.com
SCIENCE DIRECT®
ELSEVIER
Engineering Geology 68 (2003) 67–101
ENGINEERING GEOLOGY
www.elsevier.com/locate/enggeo

Seasonal movement of the Slumgullion landslide determined from Global Positioning System surveys and field instrumentation, July 1998–March 2002☆

J.A. Coe[a,*], W.L. Ellis[a], J.W. Godt[a], W.Z. Savage[a], J.E. Savage[b], J.A. Michael[a], J.D. Kibler[a], P.S. Powers[a], D.J. Lidke[a], S. Debray[c]

[a]US Geological Survey, Denver Federal Center, MS 966, Denver, CO, USA
[b]Department of Geology and Geological Engineering, Colorado School of Mines, Golden, CO, USA
[c]Département Géotechnique, Institut Des Sciences Et Techniques De Grenoble, Grenoble, France

Received 22 January 2002; received in revised form 3 May 2002; accepted 23 May 2002

Abstract

Measurements of landslide movement made by global positioning system surveys and extensometers over a 3.5-year period show that the Slumgullion landslide in the San Juan Mountains of southwest Colorado moved throughout the monitoring period, but that daily velocities varied on a seasonal basis. Landslide velocities peaked in the early spring and summer in response to snowmelt and summer thunderstorms, respectively. Velocities were slowest in mid-winter when air and soil temperatures were coldest and precipitation was generally low and/or in the form of snow with a low water content. We hypothesize that the seasonal variability in velocities is due to ground-water levels and corresponding pore pressures that decrease when surface water is unavailable or cannot infiltrate frozen landslide material, and increase when surface water from melting snow or rainfall infiltrates unfrozen landslide material. We also suggest that patches of bouldery debris and fractures (created by continuous movement of the landslide) are conduits through which surface water can infiltrate, regardless of the frozen or unfrozen state of the landslide matrix material. Therefore, the availability of surface water is more important than landslide temperature in controlling the rate of landslide movement. This hypothesis is supported by field instrumentation data that show (1) landslide velocities coinciding with precipitation amounts regardless of the depth of freezing of landslide material, (2) spring and annual landslide velocities that were greatest when the depth of freezing was also the greatest, and (3) a rapid (several weeks or less) velocity and pore pressure response to rainfall.

The persistent, but seasonally variable movement of the landslide, fits the bathtub model for landslide movement described by Baum and Reid [Baum, R.L., Reid, M.E., 2000. Ground water isolation by low-permeability clays in landslide shear zones. In: Bromhead, E.N., Dixon, N., Ibsen, M.-L. (Eds.), Landslides in Research, Theory and Practice. Proc. 8th Int. Symp. on Landslides, Cardiff, Wales, vol. 1, 139–144]. In their model, the landslide is isolated both mechanically and hydrologically from adjacent materials by low permeability clays. These clays cause the landslide to retain water. Our data support this model

☆ The use of trade, product, industry, or firm names is for descriptive purposes only and does not imply endorsement by the US Government.

* Corresponding author. Tel.: +1-303-273-8606; fax: +1-303-273-8600.
E-mail address: jcoe@usgs.gov (J.A. Coe).

PII: S0013-7952(02)00199-0

by suggesting that pore pressures at the basal landslide surface are always adequate to maintain landslide movement and that any infiltration of water at the surface of the landslide is adequate to rapidly increase landslide velocity.

Keywords: Slumgullion; Landslide; Colorado; GPS; Extensometer; Monitoring; Seasonal movement; Snowmelt; Rainfall; Monsoon; Pore pressure

1. Introduction

The Slumgullion landslide represents an extraordinary, long-term record of surface change in the San Juan Mountains of southwestern Colorado (Fig. 1). It is about 6 km long, 200–1000 m wide, and ranges in elevation from about 2750 to 3650 m. It has moved at least three times during the last 1300 years (Madole, 1996). About 700 years ago, the landslide dammed the Lake Fork of the Gunnison River and formed Lake San Cristobal, the second largest natural lake in Colorado. The currently active part of the landslide (Fig. 2) is about 3.9 km long, ranges in elevation from about 2950 to 3650 m, has an estimated volume of 20×10^6 m^3 (Parise and Guzzi, 1992), and has probably been moving for about 300 years (Varnes and Savage, 1996a). The average slope of the active part of the landslide (not including the headscarp) is about 8°.

The headscarp of the landslide (Fig. 2a) occurs in Tertiary volcanic rocks of the Uncompahgre–San Juan caldera complex (Lipman, 1976; Sharp et al., 1983; Diehl and Schuster, 1996). The upper part of the scarp is composed of vesicular basaltic lava flows and welded ash-flow tuffs, whereas the lower part of the scarp is composed of andesitic flows that have been highly altered by acid-sulfate hydrothermal alteration (Diehl and Schuster, 1996). Hydrothermal fluids weakened the andesitic rocks by altering primary minerals (plagioclases and biotite) to clays (kaolinite and smectite) and iron-rich potassium sulfate minerals (alunite and jarosite). Tertiary volcanic rocks and Quaternary landslide and glacial deposits lie along the flanks of the landslide (Lipman, 1976).

Materials that make up the active landslide are heterogeneous, but typically consist of a yellow, sandy-silty-clay with scattered patches of bouldery debris, reddish-brown and purple clay, and pond and stream sediments. Much of the clay-rich landslide material has a medium to high plasticity and high swelling potential (Chleborad et al., 1996). Perennial and intermittent springs, streams, and ponds are on the surface of the landslide. Vegetation on the landslide consists predominantly of deformed, open stands of Englemann spruce and aspen. Vegetation surrounding the landslide consists of closed stands of conifers and aspen. On the basis of elevation and observed vegetation, the landslide is in the montane and subalpine ecological zones as defined by Löve (1970).

Although the active landslide has been observed and studied since the late 1800s (e.g., Endlich, 1876; Atwood and Mather, 1932; Crandell and Varnes, 1961; Varnes and Savage, 1996b), with the exception of limited observations by Savage and Fleming (1996), little is known regarding the nature and magnitude of the landslide movements in response to short-term and seasonal variations in meteorological conditions, and nothing is known regarding the effect of surface and subsurface water on landslide movements. Previous studies (Crandell and Varnes, 1961; Powers and Chiarle, 1996; Smith, 1996; Baum and Fleming, 1996; Savage and Fleming, 1996; Fleming et al., 1999) have documented annual rates of movement ranging from 0.5 m/year at the head and toe of the landslide and up to about 6 m/year in the narrowest part of the landslide (Fig. 2b). Several additional studies have documented movements over shorter periods of time. Jackson et al. (1996) used global positioning system (GPS) surveys to measure daily velocities of up to 1 cm/day at six locations during a 4-day period in June, 1993. Savage and Fleming (1996) measured velocities over a 9-month period (April 1993–January 1994) at three locations on the landslide and reported an increase of movement rate in the spring, presumably with spring snowmelt and thawing of the landslide surface. They inferred that variations in velocity over the course of a year were in part due to hydrologic controls. However, they suggest that, because of the remarkable long-term record of rela-

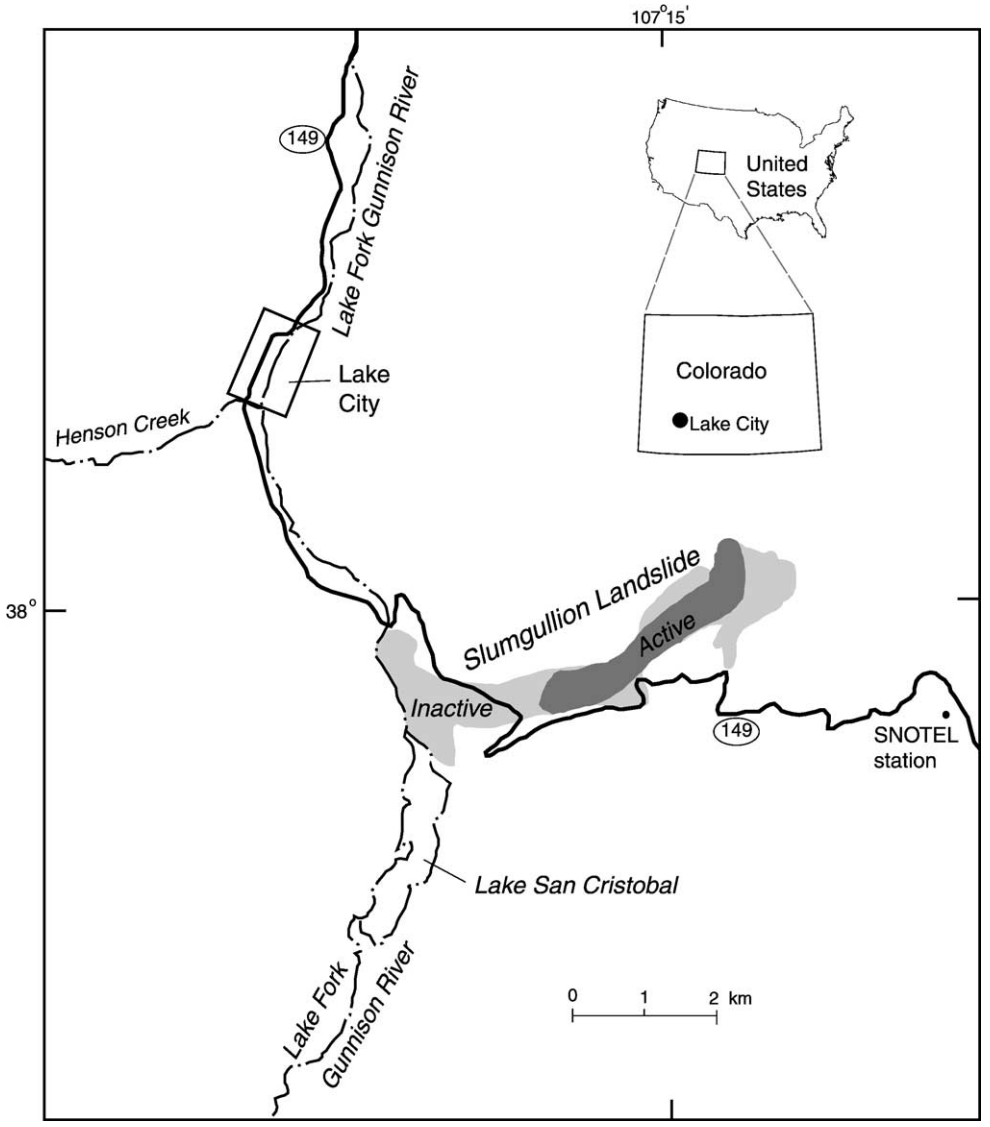

Fig. 1. Map showing the active and inactive parts of the Slumgullion landslide and the location of the Slumgullion SNOTEL meteorological station. Colorado State Highway 149 is also shown.

tively constant movement, the landslide might contain various internal mechanisms to counterbalance changing meteorologic and hydrologic conditions that act to decrease or increase landslide movement. For example, high ground-water pressures following a wet winter might be equilibrated through a network of springs, which would bleed off excess water and decrease ground-water pressures. Although some preliminary mapping of springs and sinks has been completed (Fleming et al., 1999), the overall hydrology of the landslide and its relation to movement and meteorology is unknown.

In 1998, Brigham Young University (BYU) and the US Geological Survey (USGS) began work on a National Aeronautics and Space Administration (NASA)-funded study of the Slumgullion landslide. The objectives of the study are to: (1) measure movement of the entire active part of the landslide on a

seasonal basis using GPS, and an airborne, interferometric capable, Synthetic Aperture Radar (INSAR); (2) attempt to correlate the measured movement with observed temperature, rainfall, snow depth, and ground- and surface-water levels and pressures, (3) evaluate the use of INSAR for monitoring the movement of landslides by confirming that a static velocity field surrounds the landslide and by comparing INSAR data to simultaneous measurements at GPS points, and (4) develop a model for landslide deformation based on all of the combined data. Between June and October 2001, BYU acquired five sets of INSAR data over the landslide. These data are currently (April 2002) being processed. The USGS is responsible for monitoring landslide movement using GPS, as well as monitoring hydrologic and meteorologic fluctuations on the landslide.

The purpose of this report is to present an interpretation of seasonal landslide movement determined by GPS and extensometer observations during a 3.5-year period between July 1998 and March 2002. Our interpretation of seasonal movement is in the context of hydrologic and meteorologic data collected using field instrumentation during the same time period. We also compare annual movements measured between 1998 and 2002 to previously measured annual movements. Below, we briefly describe the meteorological setting of the landslide and the GPS and field instru-

a

Fig. 2. Active part of the Slumgullion landslide. (a) Photograph taken looking to the northeast from Highway 149 on April 13, 2001. Active toe at edge of view in lower left. (b) Map showing structural elements, contours of mean annual movement, GPS base stations, control points, and monitoring points. Map modified from Baum and Fleming (1996).

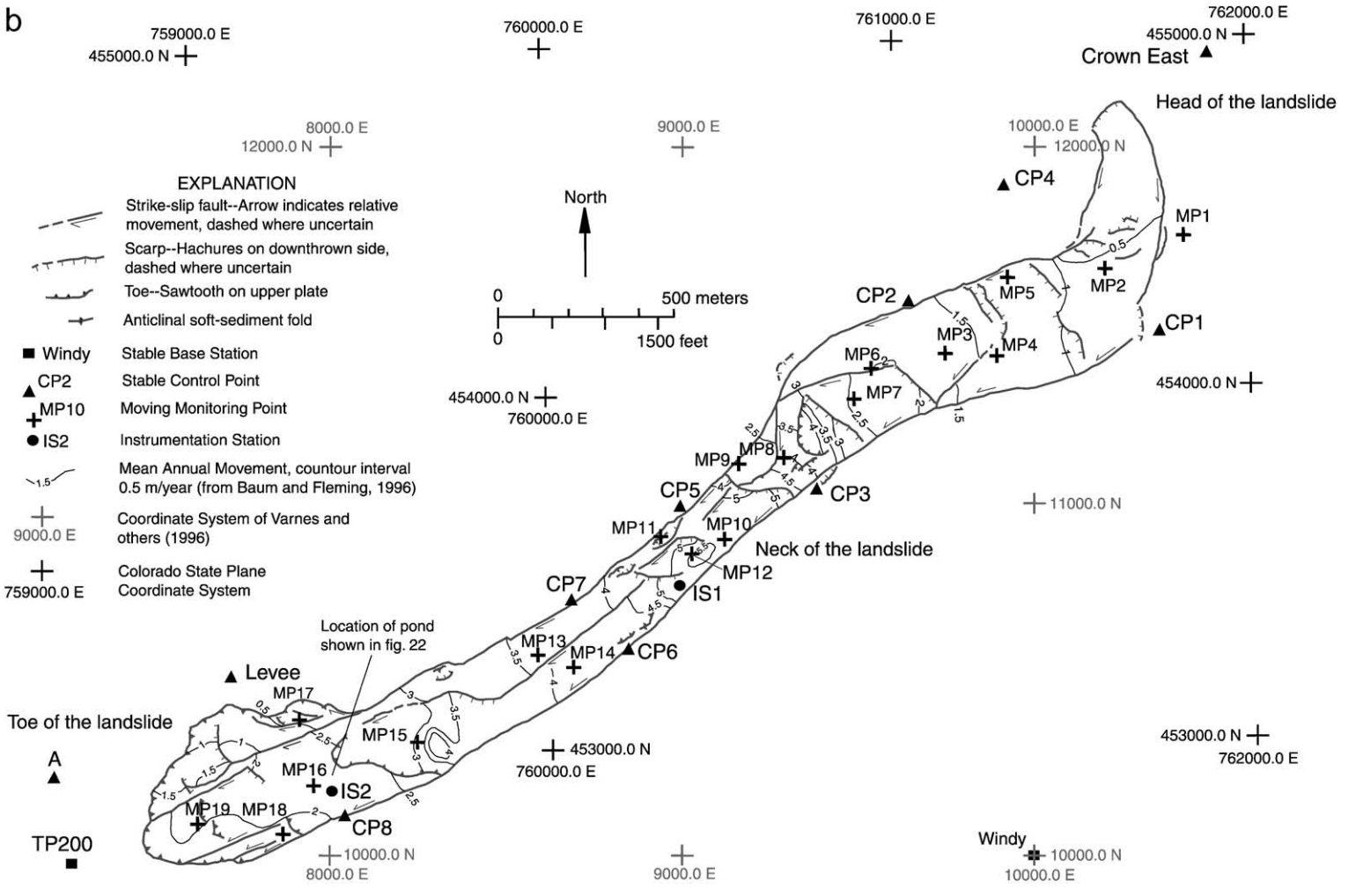

Fig. 2 (*continued*).

mentation methods used, then describe the results from monitoring, and conclude with our interpretation of seasonal movement.

2. Meteorological setting

A SNOTEL (SNOwpack TELemetry) weather station located about 4 km southeast of the head of the landslide at an elevation of 3487 m (Fig. 1) provides an overview of meteorological conditions in the area. The SNOTEL station is part of an automated network of stations, operated by the Natural Resources Conservation Service of the US Department of Agriculture, which collect snowpack and related climatic data in the western United States. Unpublished data collected between October 1980 and March 2002 at the SNOTEL station near the landslide reveal the following observations about precipitation and temperature conditions in the area. Annual precipitation is compiled per water year (WY), which is October 1–September 30, and thus, for example, WY 1999 refers to the period from October 1, 1998 to September 30, 1999. For WY 1981 through WY 2001, annual precipitation ranged from 500 to 900 mm. At least 60% of this annual precipitation was in the form of snow (Fig. 3). The first snowfall that accumulates on the ground usually occurs between late September and early November (Fig. 4). The maximum snow-water equivalent (the amount of water derived if snow on the ground were melted) usually occurs between mid-April and early May. May and June are typically dry and relatively warm so snow melts quickly and is completely gone by mid-May to early June. Extreme temperatures between 1980 and 2002 ranged from −33 °C on February 1, 1985 to 27 °C on July 4, 1989. Average daily temperatures ranged from −28 °C on February 1, 1985 to 16 °C on July 4, 1989.

SNOTEL data also place meteorological conditions during the period of our GPS observations and instrumental monitoring (July 1998 to March, 2002) into a historical context. These data show that precipitation during the monitoring period ranged from below mean annual precipitation in WY 2000 (584 mm, Fig. 3) to the highest on record (at the SNOTEL station) in WY 1999 (876 mm, Fig. 3). Also, at the time this report was written (April, 2002), precipitation in the first half of WY 2002 was well below average. On April 1, 2002, cumulative precipitation was the lowest on record for an April 1 date (185 mm, about 55% of average at the

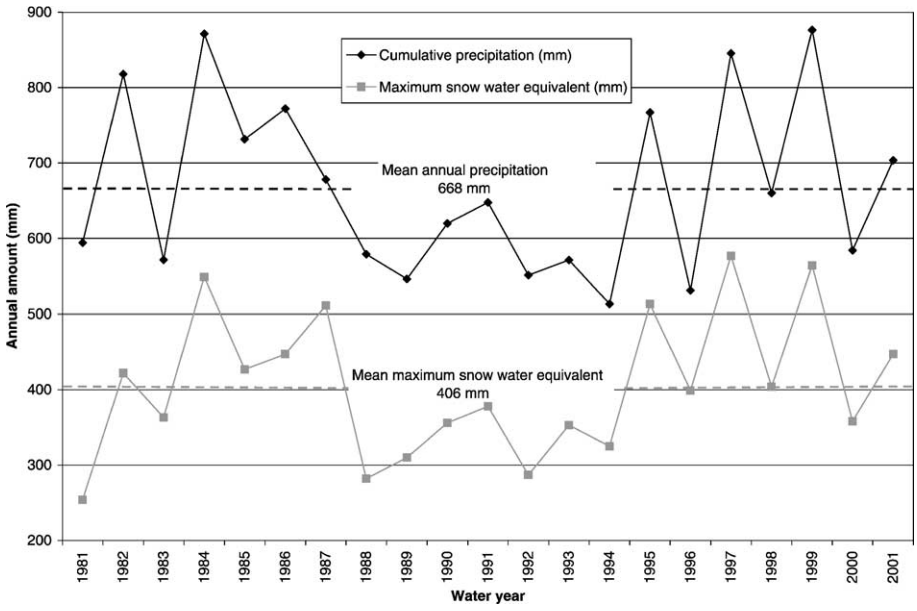

Fig. 3. Diagram showing annual precipitation and snow water equivalent measured at the Slumgullion SNOTEL station. Data from US Department of Agriculture.

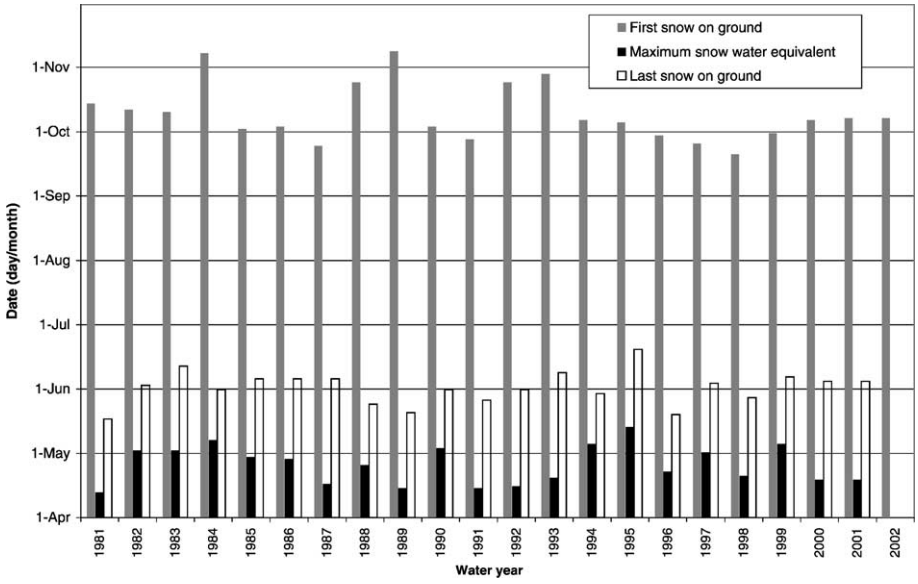

Fig. 4. Bar graph showing the times of first snowfall, last snow on the ground, maximum snow water equivalent (see text for explanation) as measured at the Slumgullion SNOTEL station. Data from US Department of Agriculture.

SNOTEL station, US Department of Agriculture, unpublished data, 2002). In WY 1999, about 60% of precipitation fell during the spring and summer (Fig. 5). In the summer of 1999, the Slumgullion landslide and the entire state of Colorado were subjected to numerous thunderstorms associated with the flow of moisture from the Gulf of California and the eastern Pacific ocean (Avery et al., 2001). This flow of

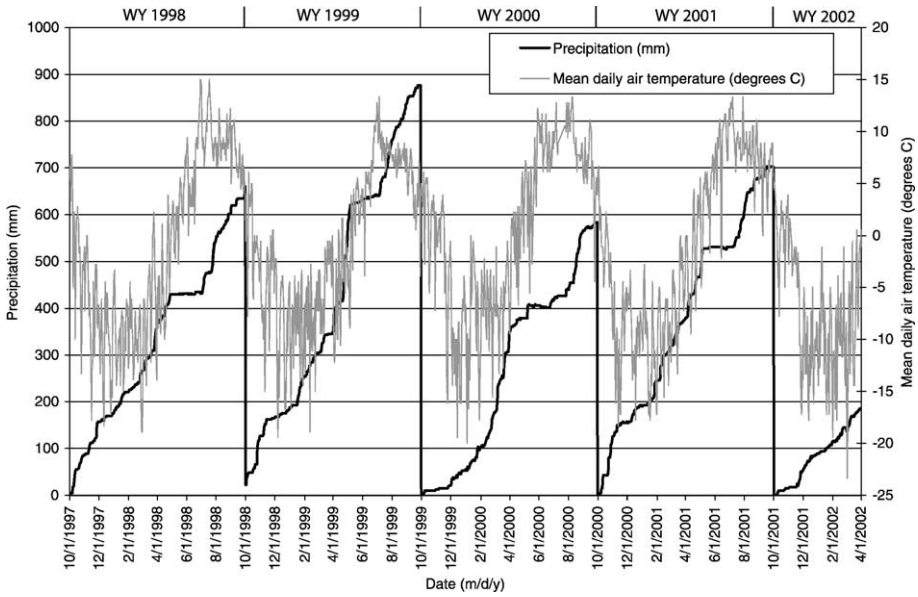

Fig. 5. Diagram showing precipitation and air temperature at the Slumgullion SNOTEL station during the monitoring period of this study. Data from US Department of Agriculture.

moisture is typically strongest in the southwestern United States in July and August and is sometimes called the southwest monsoon or North American monsoon (Hales, 1974; Hansen, 1975; Barlow et al., 1998; Avery et al., 2001). Thunderstorms associated with the monsoon in July 1999 triggered numerous and widespread landslides, debris flows, and floods throughout the state (e.g., Coe et al., 1999; Colorado Geological Survey, 1999; Avery et al., 2001), as well as several debris flows on the Slumgullion landslide (USGS, unpublished data). Similar rainstorms in August, 2001 triggered debris flows in the San Juan Mountains near Telluride about 48 km west of Slumgullion, and in the Collegiate range near Mount Princeton about 120 km northeast of Slumgullion (USGS, unpublished data).

3. Methods

3.1. Installation and distribution of control points and monitoring points

In July, 1998, 11 control points and 19 monitoring points were installed around and on the active landslide, respectively (Fig. 2b). Each control and monitoring point consists of rebar with an aluminum cap. Control points were evenly distributed in nonmoving areas around the periphery of the landslide and were commonly installed on old landslide flank ridges just outside the boundaries of the active landslide. The control points provide a stable reference frame in which to register remote sensing imagery to a local coordinate system. The 19 monitoring points were evenly distributed on the active landslide, but also strategically placed in relation to the main structural components of the landslide (Fig. 2b) and with a clear view to the sky. The clear view to the sky is necessary for reliable acquisition of the GPS signal. These points serve to record seasonal movement and form an independent data set for comparison with the results of the INSAR studies.

3.2. GPS

GPS has been previously described elsewhere (e.g., Leick, 1990; Van Sickle, 1996). Application of GPS to landslide work has also been described elsewhere (e.g., Jackson et al., 1996; Gili et al., 2000; Malet et al., 2002). Therefore, we only briefly describe the equipment, methods, and processing techniques used at Slumgullion. We refer the reader to the papers mentioned above for more detailed discussions of GPS equipment and techniques.

All control and monitoring points were surveyed using Ashtech Z-12 and Z-Surveyor, dual-frequency receivers equipped with Ashtech geodetic or marine antennas. Rapid-static GPS surveying with relative positioning was used for all points. We typically used four receivers for each survey; two receivers positioned at base stations (Windy and TP200, Fig. 2b), and two receivers roving to points on the landslide. Windy and TP200 consist of rebar with stamped bronze caps. Both stations were originally installed in the early 1990s (see Varnes et al., 1996). The WGS84 positions of Windy and TP200 were determined by a static-GPS survey in May, 1997 using a Federal Base Network Control Station (Station Designation S424, located near the Blue Mesa reservoir about 50 km north of Lake City) as a base station.

Control points were surveyed two times, in July 1998, and in July 2000. After surveying the control points in July, 2000, we discovered that one of the points (CP1, Fig. 2b) was moving. Therefore, starting

Table 1
Dates of GPS campaigns during the 3.5-year monitoring period

Dates of GPS campaigns	Days elapsed since previous campaign
July 28–29, 1998	Not applicable
October 21–22, 1998	85
January 5–6, 1999	76
March 23–24, 1999	77
May 11–12, 1999	49
July 27–28, 1999	77
November 4, 1999	99
January 5, 2000	62
March 30, 2000	85
May 16, 2000	47
July 24–26, 2000	71
September 19, 2000	55
November 16–17, 2000	59
April 12–13, 2001	147
June 7–8, 2001	56
July 20, 2001	42
August 11, 2001	22
August 28, 2001	17
October 11, 2001	44
March 5–6, 2002	146

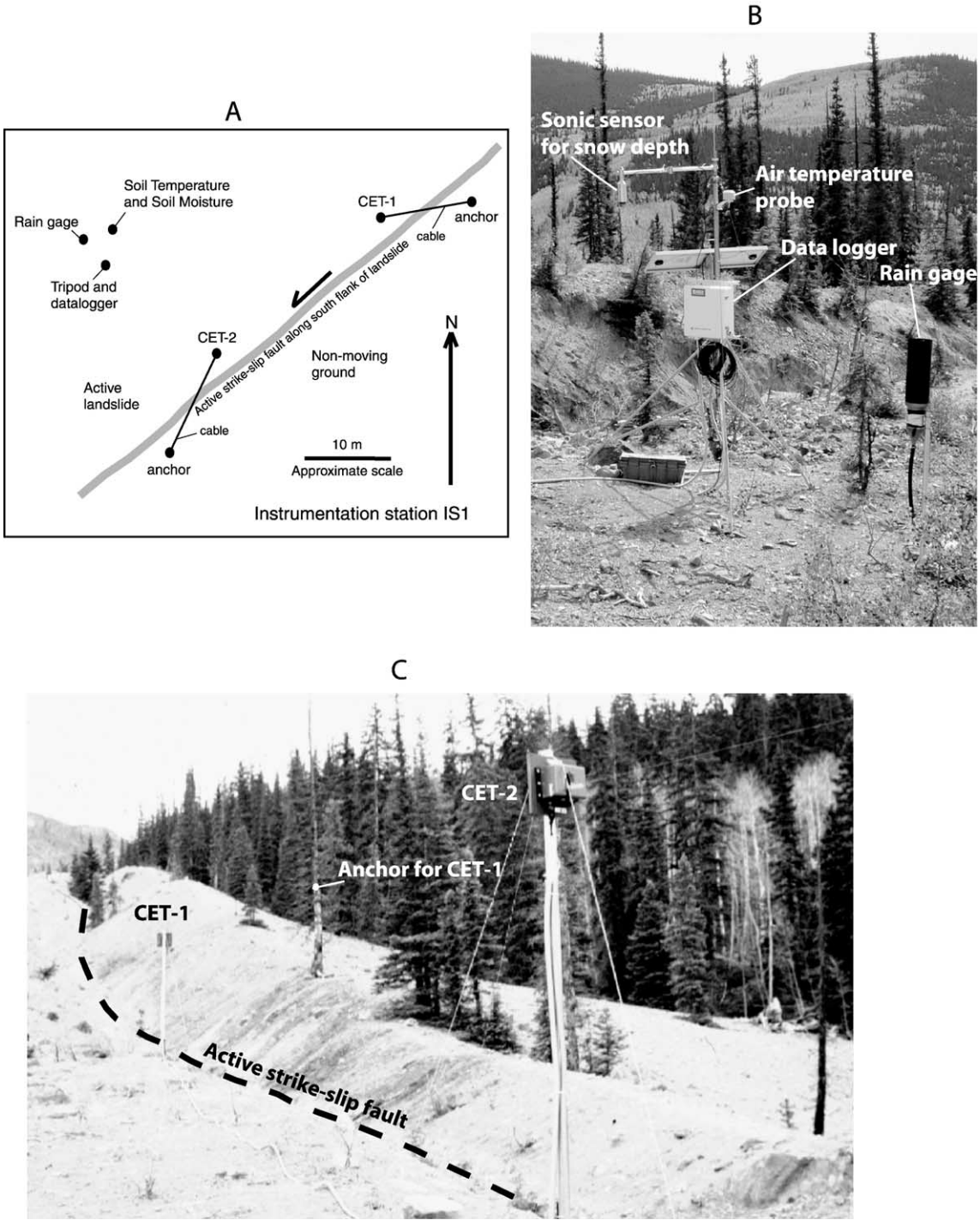

Fig. 6. Field instrumentation station IS1. (A) Sketch map showing the position of instruments with respect to landslide features. (B) Datalogger and other instruments. View to the south. Photo taken September 19, 2000. (C) Opposing CETs with cables crossing the primary strike-slip fault along the south flank of the landslide. View to the northeast. Photo taken October 22, 1998.

in July 2000, we began surveying CP1 as if it were a monitoring point. Monitoring points were surveyed during twenty 1- to 3-day field campaigns over a period of about 3.5 years (Table 1). The shortest time between field campaigns was 17 days and the longest was 147 days. The mean time between campaigns was 69 days.

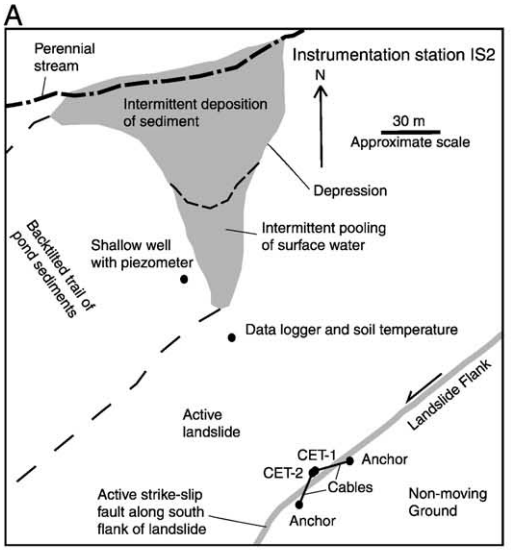

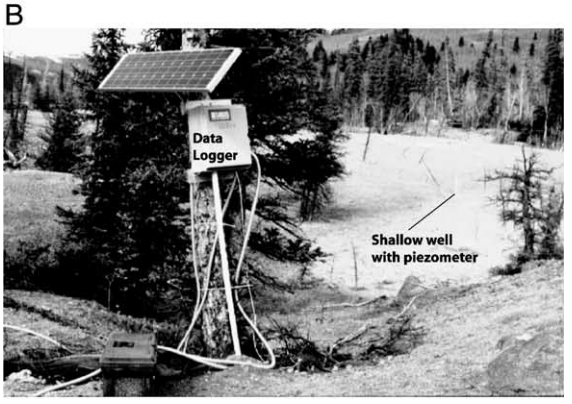

For some surveys, we were only able to use one base station. Typically, this situation was caused by problems at Windy because of its exposure to wind and solar extremes, as well as vandals. Problems included deep snow and ice covering the station, settling of tripod legs in thawing ground, dead receiver batteries, and vandalism of the station.

All GPS data were post-processed using Ashtech Precise Navigation (PNAV) software, v. 2.4.00 M. Baselines and point positions were calculated from Windy and/or TP200 for each of the measured control and monitoring points. Baselines were all less than 4 km long (Fig. 2b) so we did not remove ionosphere delay of the GPS signal as part of the processing. For surveys where two base stations were used, the calculated baselines formed a triangle with one side known (TP200 to Windy), and two sides measured (Windy to the measured point and TP200 to the measured point). The measured baselines and point positions were then refined using a least-squares adjustment contained in Ashtech PRISM software, v. 2.1. During the adjustment, the positions of Windy and TP200 were held fixed and the baselines and positions of the measured points were adjusted. In general, positions of adjusted points did not change by more than 1.5 cm horizontally and 3 cm vertically from the original (unadjusted) positions as determined from GPS data alone.

For surveys where we used one base station, unadjusted point positions as determined by GPS alone were reported as the final positions. Because we had learned that the maximum adjustments were in the range of 1.5–3 cm, our inability to perform the adjustment did not substantively change our results. Standard errors of computed point positions were derived from PNAV, in cases where point positions

Fig. 7. Field instrumentation station IS2. (A) Sketch map showing the position of instruments with respect to landslide features. (B) Datalogger with pond sediments and shallow well in the background at right. View is to the northwest. Photo taken October 23, 1998. (C) Shallow well with piezometer. Intermittent pond is in background. See hand-held radio for scale. View to the northeast. Photo taken October 11, 2001.

were not adjusted, or from the least squares adjustment, in cases where point positions were adjusted. Standard errors were less than or equal to 1 cm in horizontal and 1.5 cm in vertical.

After surveying, post-processing, and adjustment, coordinate positions for all measured points were transformed into the North American Datum of 1983 and then projected into the Colorado State Plane, southern zone, coordinate system using PRISM software. Ellipsoid heights were transformed into heights in the North American Vertical Datum of 1988 using PRISM software and the GEOID96 model provided by the US National Geodetic Survey. Coordinates and errors of points surveyed between July 1998 and July 1999 are reported in Coe et al. (2000a). Coordinates and position errors of points surveyed between July 1999 and March 2002 will be released as a USGS Open File Report.

3.3. Field instrumentation

To further examine seasonal variations in landslide movement and to correlate variations in movement to local meteorological and hydrologic conditions, two instrumentation stations were installed on the landslide (stations IS1 and IS2, Fig. 2b) during late summer and fall of 1998. Both stations are equipped with a Campbell Scientific CR10x data logger powered by solar panel and battery, and have operated since September 1998. Both stations are near the south flank of the landslide. Station IS1 (Fig. 6A) is at the neck of the landslide where velocities are the greatest. Station IS2 (Fig. 7A) is located closer to the toe of the active landslide where velocities are slower. Instruments at IS1 monitor displacement, air temperature, soil temperature and soil moisture at two different depths, precipitation, and snow depth (Fig. 6B,C). Instruments at IS2 monitor displacement, soil temperature at one depth, and shallow ground-water pore pressure (Fig. 7B,C). Measurements are recorded hourly at each station.

3.3.1. Station IS1

At station IS1, displacement along the primary strike-slip fault at the south flank of the landslide is monitored using two PSI-Tronix displacement trans-

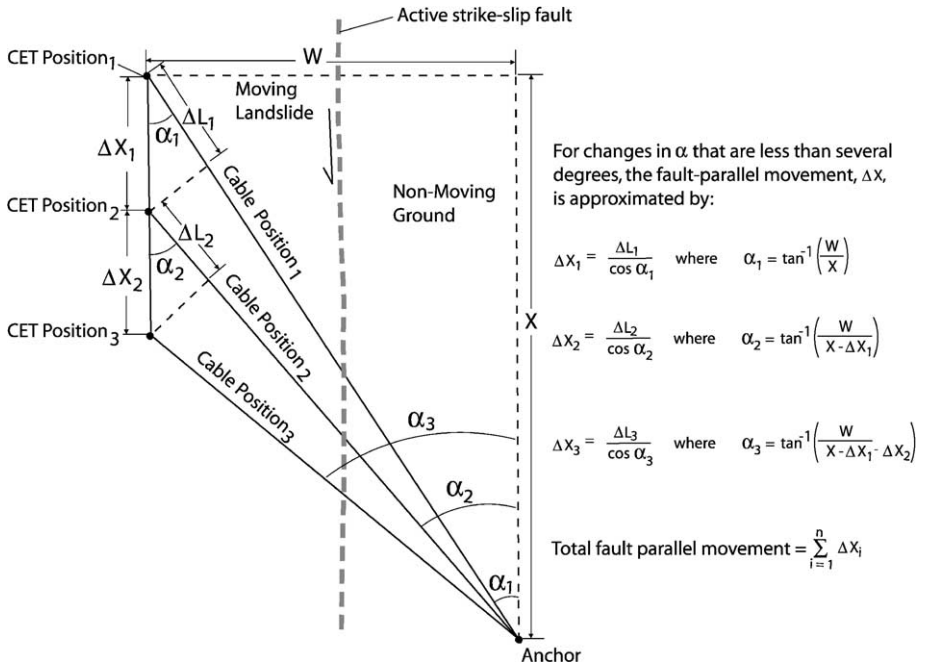

Fig. 8. Diagram showing the correction used to convert incremental changes in CET cable length (ΔL) to fault-parallel (flank-parallel) displacement (ΔX). Modified from Savage and Fleming (1996).

ducers. These transducers are commonly referred to as wire extensometers or, as in this paper, cable extension transducers (CETs). The CETs are located on the landslide and the extension cables are anchored on the nonmoving ground on the south side of the landslide (Fig. 6C). The CETs are configured in opposing directions such that the cable on one instrument (CET-1) extends and the other (CET-2) retracts as movement occurs. The CETs each have a range of 7.6 m and a manufacturer's stated accuracy of 0.25% of the range. As configured for this study, the resolution of the displacement monitoring is approximately 0.25 cm. Because the extension cables cross the strike-slip fault at an angle, the measured displacements (changes in cable length) underestimate the actual displacement parallel to the fault (i.e., the south flank of the landslide). Previous work by Gomberg et al. (1995) documented that landslide displacement near the south flank is essentially parallel to the flank. In order to derive the displacement parallel to the south flank, a geometric correction must be applied to the extensometer data. In order to be accurate, this correction must be applied incrementally, for small amounts of landslide movement, because the angle between the extension cable and the flank continually changes as the landslide moves. Therefore, for each hourly increment of movement, the change in length of the extension cable was divided by the cosine of the angle between the cable and the flank to yield the fault-parallel displacement (Fig. 8). This increment of displacement was then used to calculate the new angle for calculating the next increment of flank-parallel displacement as shown in Fig. 8. The total flank-parallel displacement throughout the monitoring

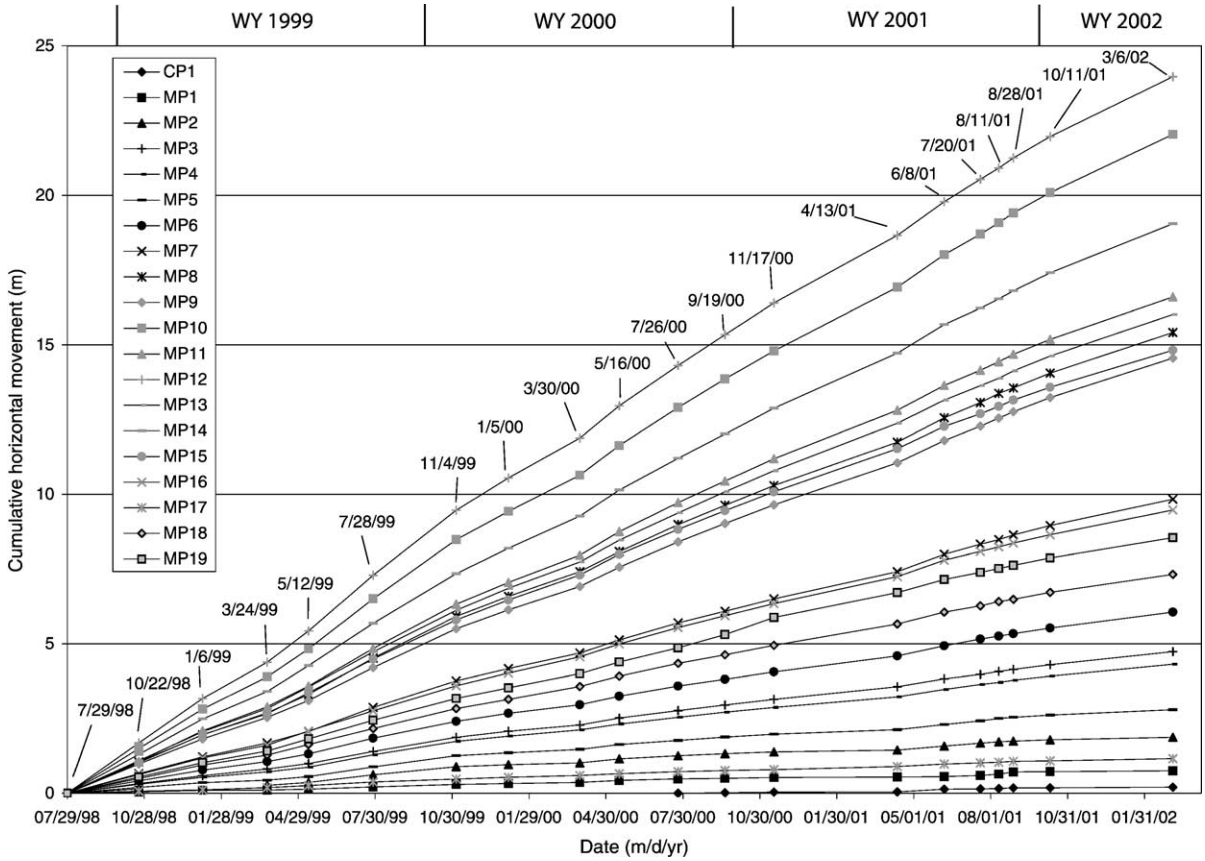

Fig. 9. Diagram showing cumulative horizontal movement of GPS monitoring points. Ending dates of GPS campaigns are shown.

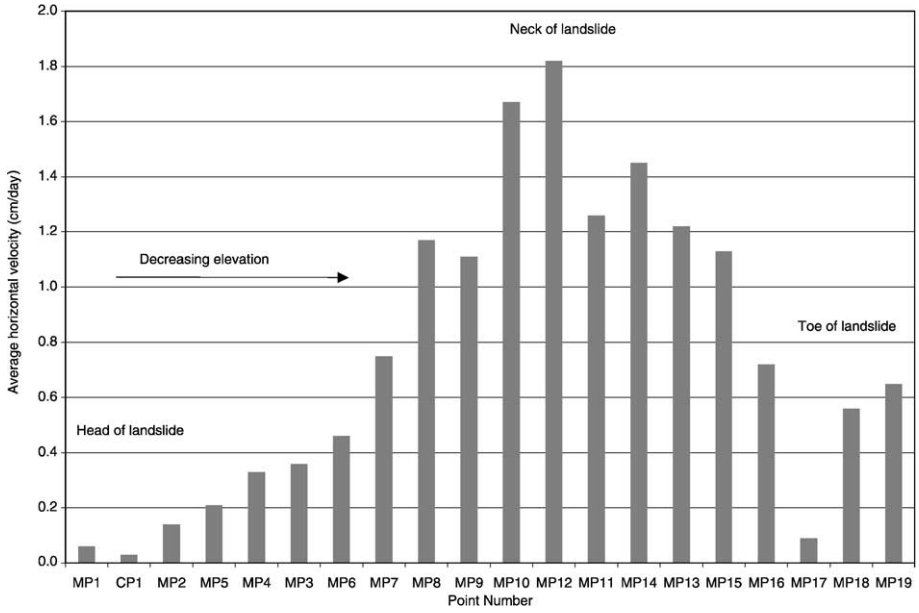

Fig. 10. Bar graph showing the average daily horizontal velocity of each GPS monitoring point. Data are averaged over the entire monitoring period.

period is the cumulative sum of the individual displacements (Fig. 8). This procedure was used to correct all extensometer data. Thus, all of the extensometer displacements described below are displacements parallel to the south flank of the landslide at each measurement site.

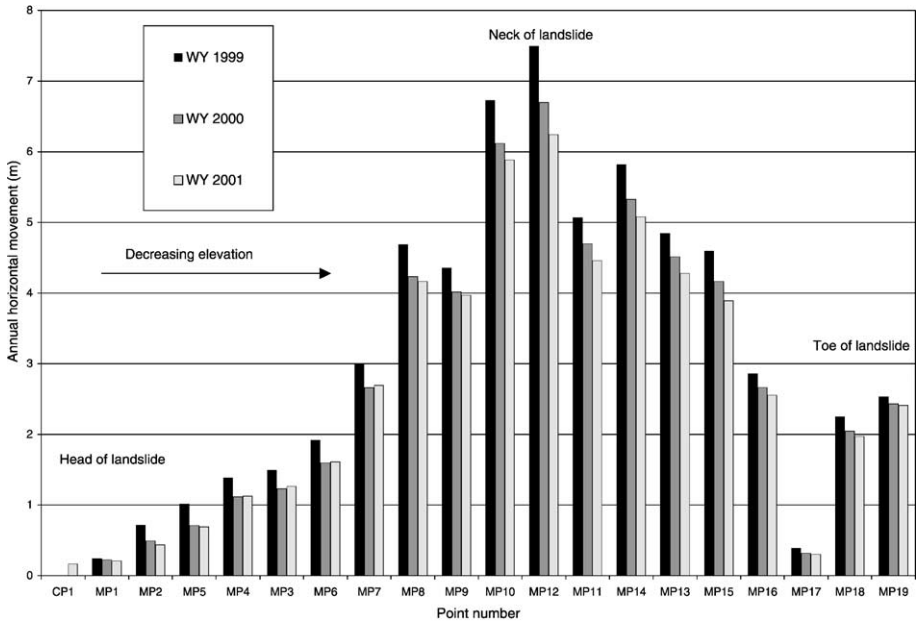

Fig. 11. Bar graph showing the annual horizontal movement of GPS monitoring points in each WY. Location of monitoring points shown in Fig. 2b.

Air and soil temperatures are monitored by Campbell Scientific model 107 temperature probes. The air temperature sensor is housed in a solar radiation shield mounted on the data logger tripod approximately 2.7 m above the ground surface (Fig. 6B). The two soil temperature probes are installed at 0.2 and 1.0 m below the landslide surface near the data logger tripod (Fig. 6A). The probes have a manufacturer's stated accuracy of $\pm 0.4^{\circ}$ C. Snow depth is monitored by a Campbell Scientific SR50 sonic ranging sensor (stated accuracy of ± 1 cm) suspended from a horizontal arm mounted on the data logger tripod. Precipitation is monitored using a Texas Electronics model TE525WS tipping-bucket rain gage equipped with a Campbell Scientific model CS705 snowfall adapter. The snowfall adapter consists of an antifreeze reservoir and associated hardware configured so that snowfall can be captured and measured at nearly the same time that it occurs, even though air temperatures may be below freezing.

Soil moisture conditions at the station are estimated using two different measuring techniques. The soil water potential, or soil tension, is estimated using two Watermark model 200 sensors manufactured by Irrometer Company. The Watermark sensor is an electrical resistance device, consisting of two concentric electrodes embedded in a granular matrix material. The device was developed primarily for agricultural applications and has been empirically calibrated to yield estimates of soil tension (Eldredge et al., 1993). Because the calibrations are empirical and based on testing in limited soil types, the soil tension values derived from

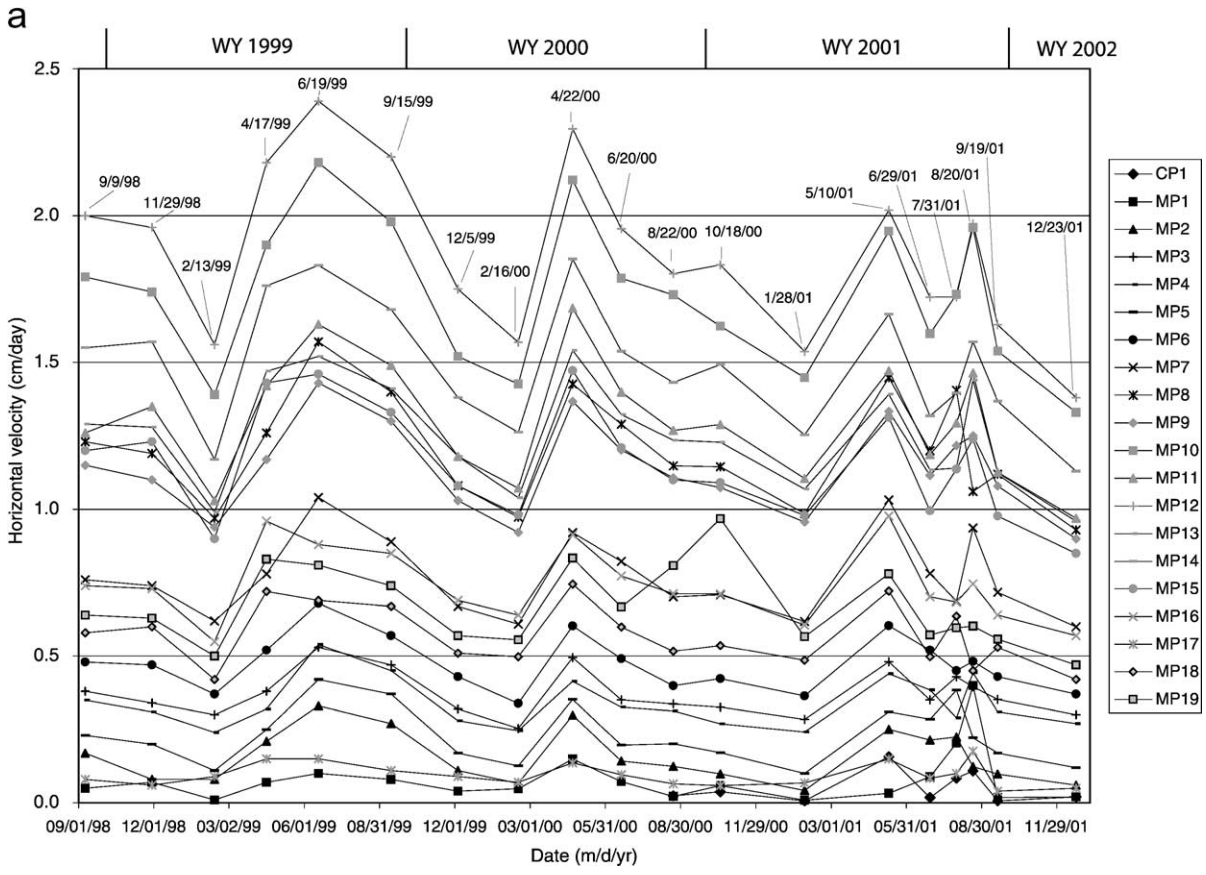

Fig. 12. Diagram showing average daily velocities of GPS monitoring points. Dates shown are the mid-points between GPS observations. (a) Velocities during the entire monitoring period. (b) Velocities during WY 2001.

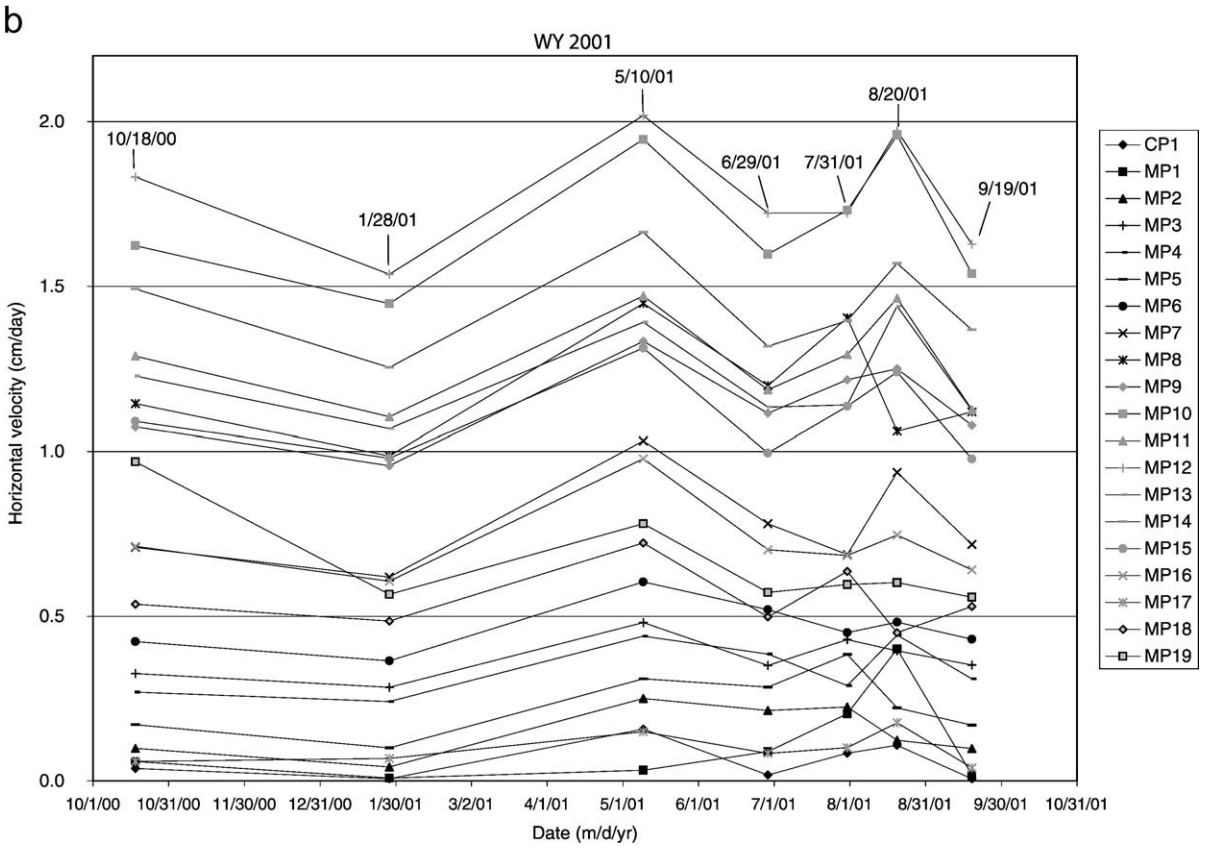

Fig. 12 (*continued*).

the method are considered to be qualitative estimates. Low values of soil tension (less negative values) in the range of 0 to − 10 kPa are generally indicative of saturated soil conditions. Values of − 100 to − 200 kPa are indicative of very dry soil conditions. Because the Watermark sensors require a temperature measurement to properly convert instrument response to soil-tension values, they are emplaced at the same depths as the soil temperature probes (0.2 and 1.0 m).

The volumetric water content at the station is estimated using a Campbell Scientific model CS615 water content reflectometer. Volumetric water content is the volume of liquid water per volume of soil. The water content reflectometer operates using a principal similar to that used by time-domain reflectometry (TDR) to determine soil moisture. The water content is derived from the effect of the changing dielectric constant of the surrounding soil on electromagnetic waves propagating along a wave-guide buried in the ground. Because the dielectric constant of soil is predominantly dependent on water content, the method provides a fairly accurate estimate of water content. Campbell Scientific claims an accuracy of ± 2% for a wide range of soil types, but the effects of high clay content or soil electrical conductivity can also have a potentially significant effect on the accuracy. Because these effects are not well defined at station IS1, the accuracy of the method in the soils at IS1 is uncertain. Accordingly, the measured water content values must be considered estimates. The values obtained, however, seem quite reasonable with respect to field observations and typical ranges of volumetric soil-water contents (e.g, Chleborad et al., 1996). The water content reflectometer is placed at a depth of 0.2 m near the same location as the 0.2 m deep Watermark sensor.

3.3.2. Station IS2

At station IS2 (Fig. 7), displacement parallel to the south flank of the landslide is monitored using the same configuration of extensometers (CETs) as at IS1. Soil temperature is monitored with a Campbell Scientific model 107 temperature probe buried at a depth of 0.5 m.

Pore pressure is monitored using a piezometer installed in an augered well near the edge of a closed depression that periodically pools water during spring snowmelt and during and after periods of intense rainfall (Fig. 7A). The well is in pond sediments (fine sand and silt) and is 7 cm in diameter and 2.2 m deep (Fig. 7B,C). The piezometer is an electrical strain-gage pressure transducer housed within a PVC casing that is 2.5 cm in diameter. The bottom 0.2 m of the PVC casing was slotted, covered with a cloth filter, and filled with coarse sand. The pressure transducer was placed on top of the sand fill at a depth of 2.0 m. The bottom 0.6 m of the annulus between the wall of the well and the PVC casing was filled with coarse sand and the remainder of the hole up to the ground surface was filled with a bentonite seal. The pressure transducer is vented to the atmosphere to eliminate the effects of barometric pressure variations from the pore-pressure measurements.

4. Results

4.1. Landslide movements determined by GPS observations

4.1.1. Cumulative and annual movement

All monitoring points (including CP1) moved between each GPS survey (Fig. 9). Total movement (combined horizontal and vertical movement) was largely dominated by the horizontal component. Cumulative horizontal movement over the monitoring period ranged from 0.8 m at MP1 at the head of the landslide, to about 24 m at MP12 in the neck of the landslide (Fig. 9). Average daily velocities over the entire monitoring period ranged from less than 0.1 cm/day at MP1 and CP1 to about 1.8 cm/day at MP12. In a general sense, cumulative movement and average horizontal velocities are smallest near the head and toe of the landslide and increase to a peak at the central, narrowest part (neck) of the landslide (Fig. 10). This movement pattern is consistent with that observed previously by Smith (1996) and Powers and Chiarle (1996). Cumulative vertical movements over the monitoring period ranged from about 0.11 m at MP1 to 4.54 m at MP10. All points, except MP16, moved downward (elevations decreased). MP16 moved upward (elevation increased, see discussion below).

Annual horizontal movements at all points were greatest during the WY 1999 (Fig. 11). In general, annual movements progressively decreased from the WY 1999 to the WY 2001. Exceptions to this observation are points MP3, MP4, MP6, and MP7, where movement during the WY 2001 was greater than during the WY 2000 (Fig. 11).

4.1.2. Seasonal velocities

Velocities of individual points varied as much as 0.8 cm/day according to the season (Fig. 12a). Maximum velocities occurred between early April and late June, whereas minimum velocities occurred between early January and late February. The spring and summer portion of this pattern was observed previously (Savage and Fleming, 1996), but only at one location on the south flank in the neck of the landslide. Minimum velocities ranged from 3% to 63% of maximum velocities (Fig 13). The largest seasonal difference in velocities occurred at points near the head of the landslide (CP1, MP1, MP2, MP5) where minimum velocities were 3–24% of the maximums. The smallest seasonal differences occurred at points in or near the neck of the landslide (MP7–MP14) where the minimum velocities were 58–63% of the maximums.

In general, maximum velocities of individual points were greatest during the WY 1999 and progressively decreased in the following two WYs (Fig. 12a). In contrast, minimum velocities remained relatively stable or slightly increased in WYs 2000 and 2001, and decreased in WY 2002.

4.1.3. Velocities in WY 1999

In WY 1999, minimum and maximum velocities occurred at different times on different parts of the landslide (Fig. 12a). Minimum velocities occurred between January 6 and March 24 over the entire landslide, except at MP17, where the minimum velocity occurred between October 22 and January 6. Maximum velocities occurred between May 12 and July 28 on the upper and middle parts of the landslide (MP1–MP15)

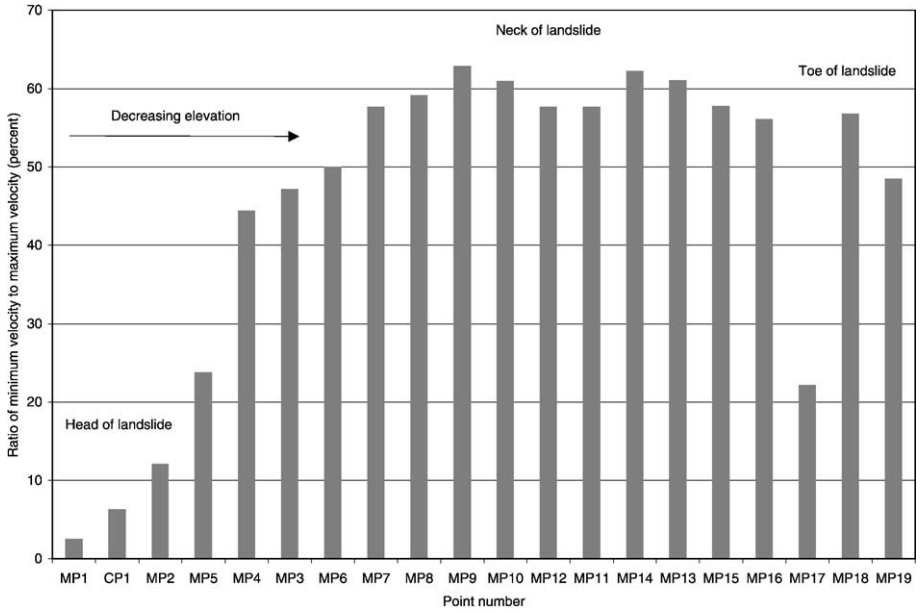

Fig. 13. Bar graph showing the ratio of minimum horizontal velocity to maximum horizontal velocity at each GPS monitoring point for the entire 3.5-year monitoring period.

and between March 24 and May 12 on the lowest part of the landslide (MP16–MP19).

4.1.4. Velocities in WY 2000

In WY 2000, minimum and maximum velocities occurred at the same times on different parts of the landslide (Fig. 12a). For the entire landslide, minimum velocities occurred between January 5 and March 30 and maximum velocities occurred between March 30 and May 16. Velocities of 13 of the 19 monitoring points progressively decreased following the peak in maximum velocities between March 30 and May 16, as had all of the points in WY 1999. However, velocities at 6 of the 19 monitoring points (MP1, MP6, MP11, MP12, MP14, and MP18) reached a low between July 26 and September 19 and then increased to a secondary peak between September 19 and November 17. The velocity of point MP19 also reached a secondary peak between September 19 and November 17, but had a low velocity between May 16 and July 26.

4.1.5. Velocities in WY 2001

In WY 2001, the velocities of points appear to be much more erratic than in previous years (Fig. 12a,b). This erratic appearance is only visible in the summer months when we performed frequent (about every 30 days) GPS surveys to coincide with INSAR flights by BYU. Because the times between these surveys were about half of the average time between surveys during the entire monitoring period (about 69 days), we detected more variation in velocities than in previous years. Compare the variations on the right side of Fig. 12b with the left side. On the left, there are three data points in 7 months, whereas on the right there are five data points in 5 months. Velocities measured during WY 1999 and WY 2000 were averaged over longer time periods and thus form smoother and more consistent cyclic patterns (as shown in Fig. 12a).

As in WY 2000, minimum and maximum velocities during the WY 2001 occurred at the same times on different parts of the landslides (Fig. 12b). For the entire landslide, minimum velocities occurred between November 17 and April 13, whereas peaks in velocities occurred during two time periods, between April 13 and June 8, and between July 26 and August 28. All points had peaks in velocities between April 13 and June 8, but peaks in velocities between July 26 and August 28 were more complex. That is, five points (MP2, MP3, MP5, MP8, and MP18) had velocity peaks between July 26 and August 11, whereas the other 15

points had velocity peaks between August 11 and August 28.

4.1.6. Velocities in WY 2002

Only two GPS surveys were performed in WY 2002 (Table 1), but velocities determined from these surveys were generally among the lowest measured during the entire monitoring period. (Fig. 12a).

4.2. Data from field instrumentation

4.2.1. Landslide displacement

Hourly displacement data measured by CETs (Fig. 14) are used to determine variations in landslide velocity from field instrumentation. These data have been processed to remove effects caused by environmental disturbances such as snow and wind load on the extension cables and by electrical disturbances of unknown origin. In several instances, the positions of the displacement lines have been adjusted to account for cable breaks or resetting of the cables because of range limitations.

More difficulty was experienced in maintaining continuous operation of the CETs at IS1 than at IS2, as evidenced by the gaps in the data at IS1. The noise in the IS1 CET-1 data after June 2000 was caused by friction from the installation of a drip ring on the extension cable. The ring caused stick-slip behavior as the cable was extended. The divergence of the IS1 CET-1 and CET-2 displacement lines is probably a result of differential displacement between the CET positions (see Fig. 6). The displacement data at IS2 are nearly continuous, except where CET-2 experienced intermittent malfunctions beginning in late July of 2001.

Total displacement during the monitoring period is about two times greater at station IS1 (17.5 m) in the neck of the landslide than at IS2 (7.9 m) at a lower elevation closer to the toe of the landslide. Displace-

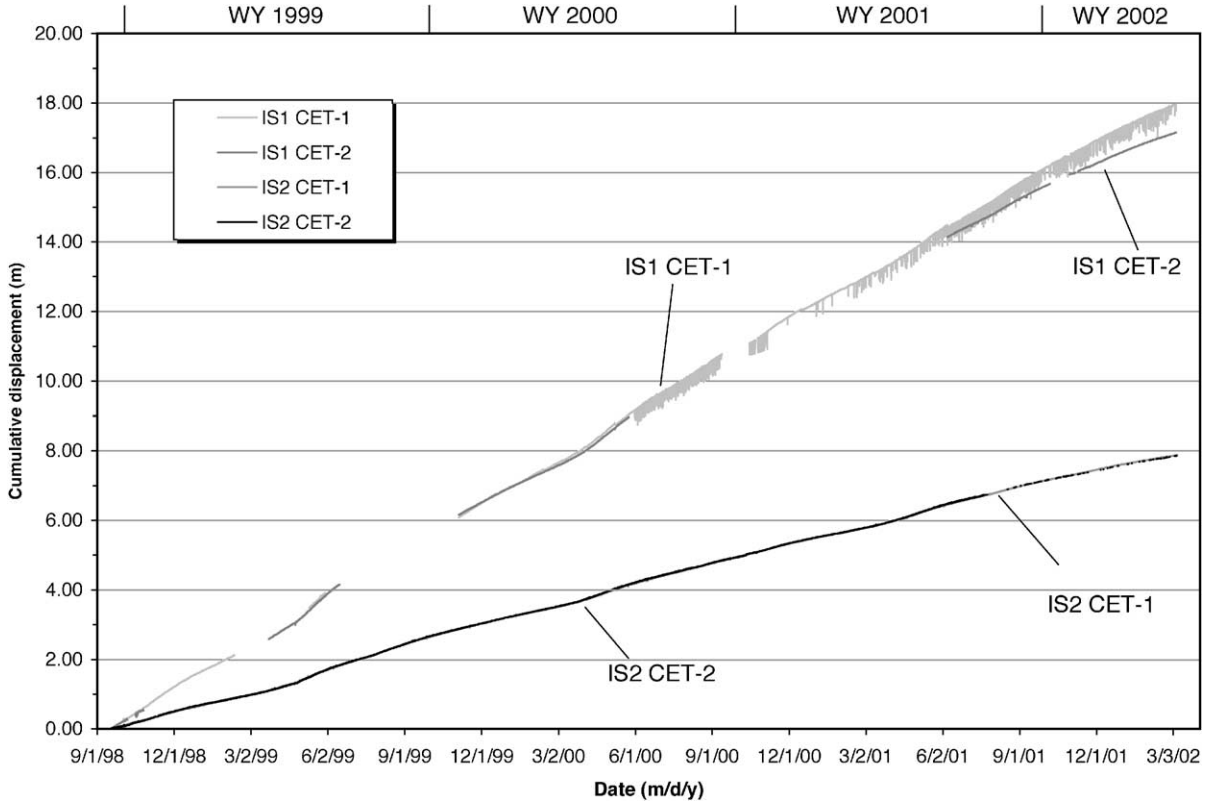

Fig. 14. Cumulative displacement measured by cable-extension transducers (CETs) across the primary strike-slip fault along the south flank of the landslide at stations IS1 and IS2. See text for further explanation of data.

ment at IS2 during WY 1999, WY 2000, and WY 2001 was 2.59, 2.29, and 2.19 m, respectively. Changes in the slope of the displacement lines indicate seasonal changes in landslide velocity. Because displacement data from IS2 are more complete than from IS1, only the IS2 data were used to derive the landslide velocities described in the sections below.

4.2.2. Landslide velocity

Velocities measured by CETs at station IS2 are shown in Fig. 15. The daily velocities were determined by calculating the slope of the respective displacement lines (Fig. 14) over 7-day periods, thus filtering the effects of signal noise and minor environmental effects. Because the configuration of the two CETs resulted in opposing effects from such external factors as snow and wind load, the velocity data from these two instruments was averaged to cancel out these effects and produce a smoother and more representative velocity line (the thick black line in Fig. 15).

The seasonal variations in landslide velocity are apparent in Fig. 15. Prominent peaks in velocity occur in the spring and summer, whereas minimum velocities occur in the winter. To compare these velocities to those measured by GPS, we use two GPS points, MP8 and MP16 (Figs. 2b and 15), which are repre-

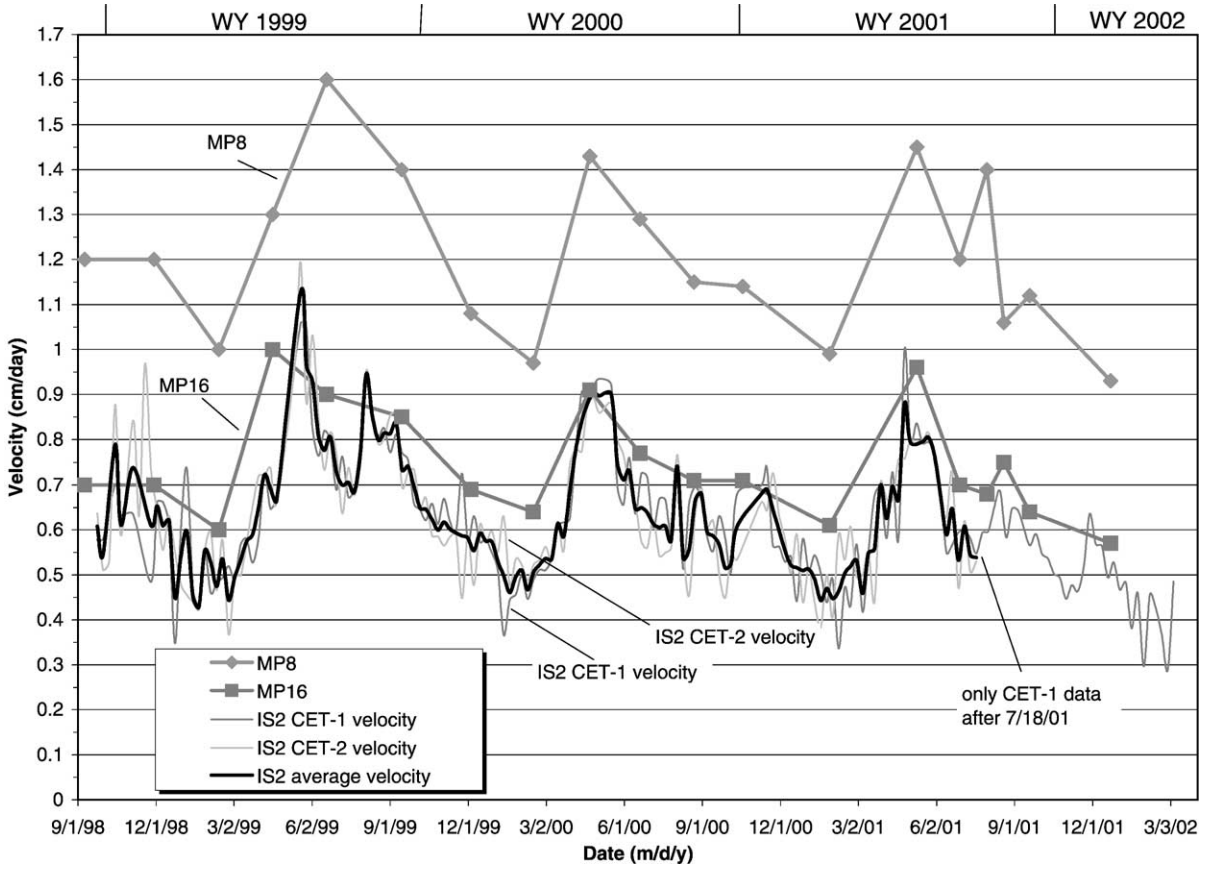

Fig. 15. Landslide velocity derived from CET measurements across the primary strike-slip fault at the south flank of the landslide at station IS2. GPS observations from monitoring points MP8 and MP16 are also shown. Velocity of MP8 is representative of the upper and middle parts of the active landslide (points MP1–MP15), and velocity of MP16 is representative of the lower part of the landslide (points MP16–MP19, see Fig. 2b). The velocities calculated for MP8 and MP16 are plotted at the mid-points between times of GPS observations. Opposing configuration of the CETs results in a mirror effect on instrument response from environmental disturbances of the extension cables. These environmental disturbances are therefore removed by averaging the results from both CETs. Only CET-1 data are shown after July 18, 2001 (in this figure and in Figs. 16–18) because CET-2 was malfunctioning and an average velocity could not be computed.

sentative of movement on the upper and lower parts of the landslide, respectively. The velocities determined by the two different methods show the same general trends, but the velocities derived from CET data provide a greater level of detail (Fig. 15). The velocity data from CETs, in conjunction with meteorological data, show that the landslide rapidly responded to changes in meteorological conditions, and that maximum velocities progressively decreased from WY 1999 to WY 2001. Minimum velocities were relatively constant from WY 1999 to WY 2001, but decreased in WY 2002. The GPS data capture the major variations in velocity but not the higher frequency (daily to weekly) variability.

4.2.3. Meteorological data and velocity variations

Seasonal variations in landslide velocity indicate that the factors controlling landslide movement are sensitive to local meteorological conditions. Meteorological conditions measured at station IS1 during the monitoring period are shown in Fig. 16.

During each WY, measured landslide velocities began to increase in mid-winter as days became longer, air temperatures gradually increased, and snow on the landslide intermittently melted (Fig. 16a). The spring increase in air temperatures triggered rapid snowmelt, which rapidly increased landslide velocity (Fig. 16a). Peak landslide velocities corresponded with the end of the snowmelt season when the snow depth had rapidly decreased from a maximum to zero (Fig. 16a). A secondary velocity peak, or multiple peaks, in velocities occurred during the monsoon season (July–August, Fig. 16b). Velocities then generally decreased to a minimum in mid-winter. An exception to this pattern occurred in the beginning of WY 2001 when a prominent peak in velocity occurred in October and Novem-

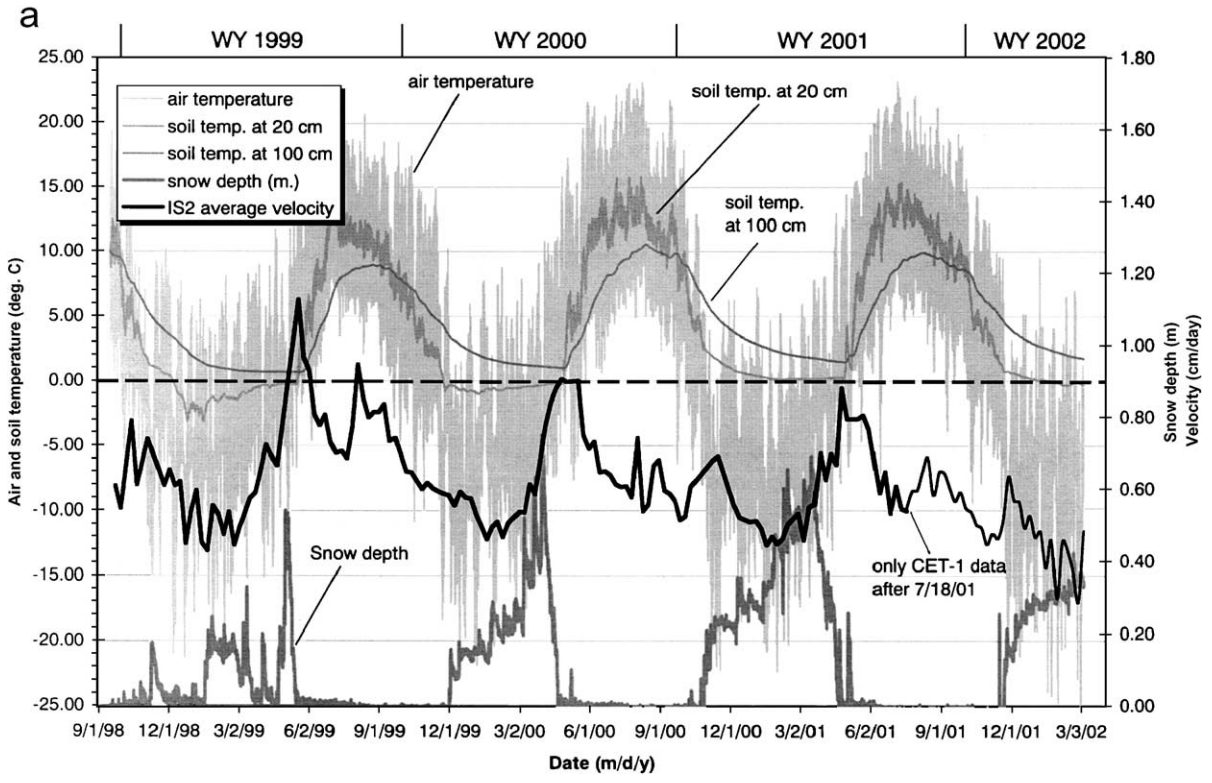

Fig. 16. Diagram showing data from instrumentation at IS1 and IS2. (a) Air temperature, soil temperature, and snow depth at IS1. Landslide velocities at IS2 are also shown. (b) Cumulative precipitation and snow depth at IS1. Landslide velocities at IS2 are also shown. Times of generally continuous snow cover are shaded and the cumulative precipitation measured during these times are shown. Note that precipitation that fell as snow was recorded at the time it fell.

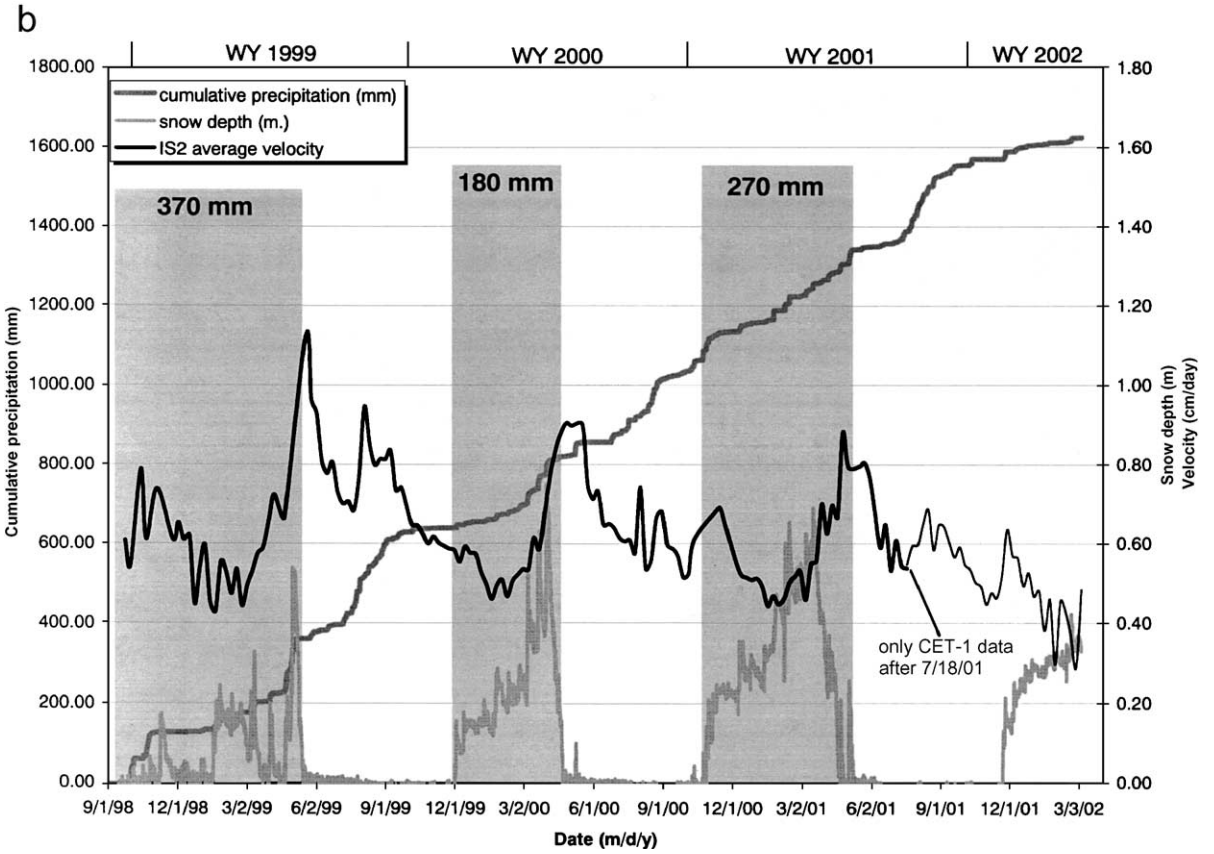

Fig. 16 (*continued*).

ber (Fig. 16b). This velocity response was probably caused by partial melting of a heavy, early season snowfall.

Cumulative precipitation measured at IS1 shows dramatic increases during July and August, particularly during the summers of WY 1999 and WY 2001 (Fig. 16b). These increases are from rainstorms related to the southwestern monsoon. Rainstorms during the monsoon periods of these two summers triggered landslides and debris flows throughout Colorado. Approximately 250 mm of rain occurred in the summer WY 1999, about 150 mm in the summer of WY 2000, and about 200 mm in the summer of WY 2001 (Fig. 16b). Late winter and early spring snows also accounted for a large part of total yearly precipitation (for example, see March–May in WY 1999 and WY 2000, Fig. 16b). These snows had a high-water content and occurred just before or during the spring snowmelt season (Figs. 4 and 16b). Total precipitation at station IS1 during WY 1999, WY 2000, and WY 2001 was 608, 406, and 520 mm, respectively. At the SNOTEL station, about 300 m higher in elevation than IS1, total precipitation during the same WYs was 876, 584, and 704 mm.

One clear difference between WYs is the duration and amount of snow cover (Fig. 16a). Snow cover during the WY 1999 winter was relatively thin compared to the WY 2000 and WY 2001 winters, but lasted longer and contained more water (Fig. 16b). This observation is consistent with data from the SNOTEL station (Fig. 3) that show the maximum snow-water equivalent in WY 1999 was greater than in WY 2000 and WY 2001. The snow pack on the landslide also melted more frequently during the WY 1999 winter than during the other winters. Air temperatures were above freezing more days during the WY 1999 winter than during the following winters (Fig. 16a). Even

though air temperatures in the WY 1999 winter were relatively warm compared with the succeeding two winters, soil temperatures were colder (Fig. 16a). During the WY 1999 and WY 2000 winters, soil temperature at 20 cm depth reached a low of −3 and −1 °C, respectively. During the WY 2001 winter, the temperature at 20 cm did not drop below freezing. Soil temperature at 1.0 m depth did not drop below freezing during any of the winters, and showed a slight warming trend in each succeeding winter. The warming of soil temperatures from the WY 1999 winter through the WY 2001 winter likely reflects the insulating effect of the snow cover, which, as stated above, increased in thickness each succeeding winter. The insulating effect of snow is clearly visible in temperature data from 20 cm, which show daily oscillations when there is no snow cover and minimal to nonexistent oscillations when there is snow cover (Fig. 16a).

In each successive WY, minimum velocities consistently occurred in mid-January, but the time of maximum velocities came earlier in each year (Fig. 16). In WYs 1999, 2000, and 2001, for example, maximum velocities occurred in mid May, early May, and late April, respectively. This pattern indicates that the duration of the snowmelt season became progressively shorter during the 3.5-year monitoring period.

Maximum yearly displacements and seasonal velocities occurred during WY 1999 when snow water content and total precipitation were higher than in other years, snow cover was thinner, but longer in duration, and soil temperature was colder. Also, in WY 1999, snow on the surface of the landslide melted more frequently than in other WYs and the snowmelt season was longer. After WY 1999, there was progressively thicker snow cover and progressively shallower freezing of landslide material in each succeeding WY

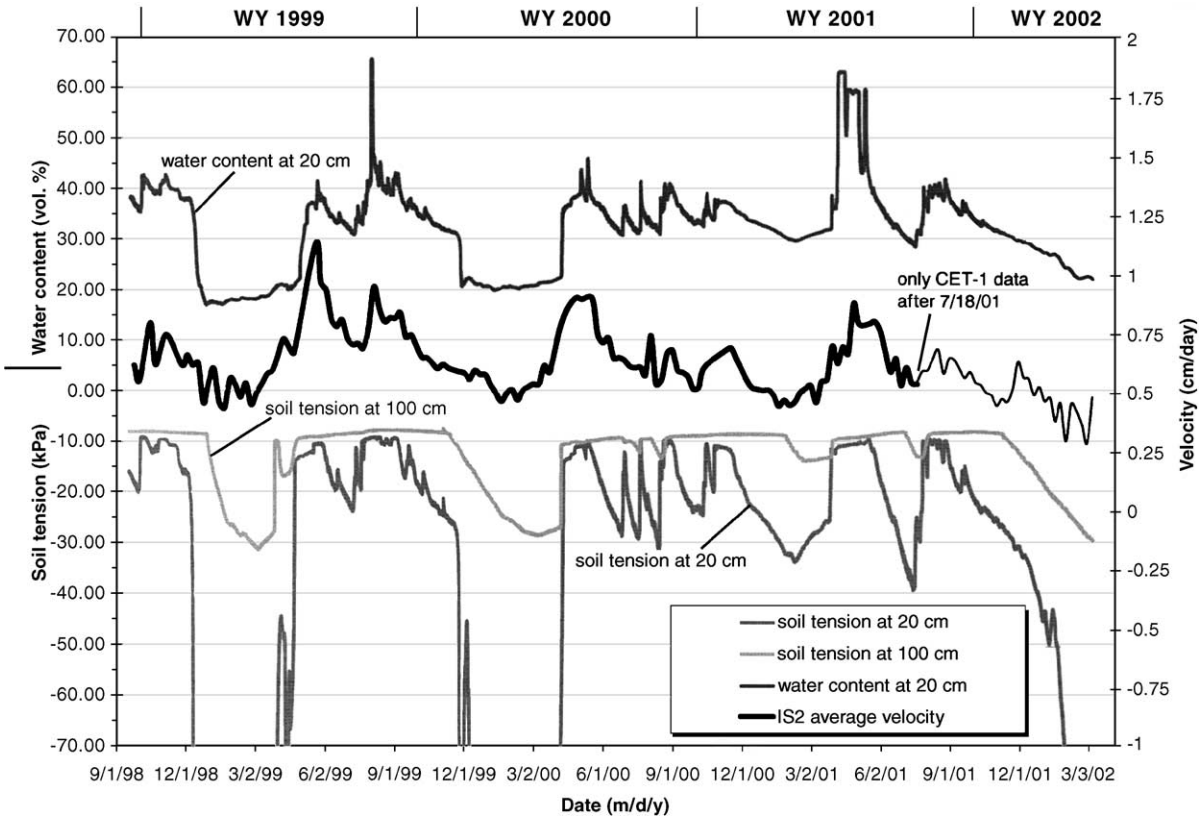

Fig. 17. Diagram showing soil-moisture conditions at station IS1. Landslide velocities at IS2 are also shown. See text for discussion of the instruments and estimated accuracies.

(through WY 2001), but total displacement and maximum velocities progressively decreased.

4.2.4. Soil-moisture and velocity variations

Soil moisture (water content and soil tension) measured at station IS1, and landslide velocities measured at IS2, are shown in Fig. 17. In general, there is a positive correlation between soil moisture and landslide velocity, that is, velocities are highest during times of high soil moisture and lowest during times of low soil moisture.

Data from the water content reflectometer and Watermark sensors show that, with the exception of the winter months, landslide material at a depth of 0.2 m had a volumetric water content that ranged from about 30% to 65% (Fig. 17) and that landslide material at depths of 0.2 and 1 m was saturated or wet (soil tensions between −7 and −30 kPa, Fig. 17). The very large decrease in soil tension readings at 20 cm depth during WY 1999, WY 2000, and WY 2002 winters (Fig. 17) correspond with periods in which soil temperatures at 20 cm dropped below freezing (Fig. 16a). The water content reflectometer data at 20 cm depth also show a pronounced decrease in volumetric water content during the same time periods. However, because these large changes in instrument readings apparently result from a change in state of the interstitial water from liquid to ice, the soil-moisture data obtained during times the ground was frozen are not considered meaningful. Decreases in soil tension also occurred at the 100 cm depth during the winter months, but soil temperatures at this depth did not drop below freezing. Less pronounced decreases in soil tension and volumetric water content occurred in the winter of WY 2001, even though freezing did not occur at or below the 20 cm depth. These observations indicate that drying occurs below frozen landslide material in the winter months, and that the magnitude

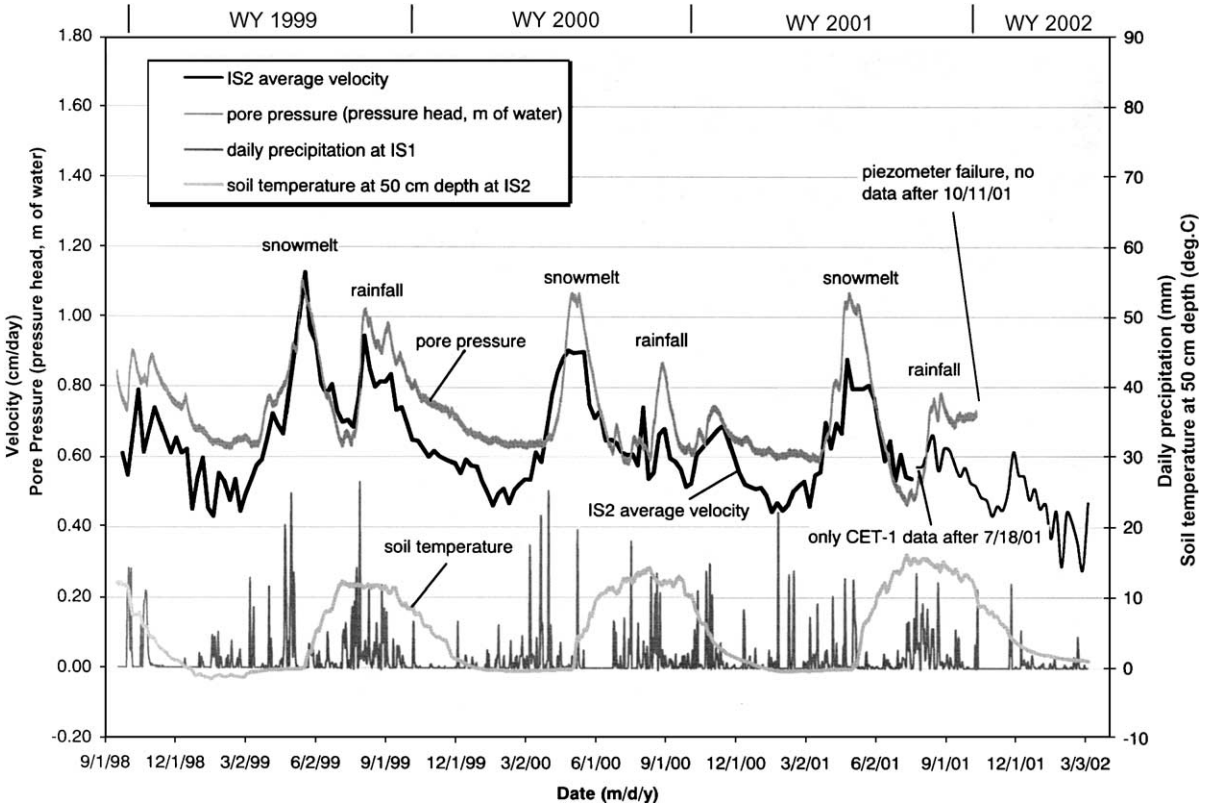

Fig. 18. Diagram showing landslide velocity, soil temperature, and pore pressure recorded at station IS2 and daily precipitation recorded at IS1. Pore pressure is shown as pressure head in meters of water above the piezometer, which is 2.0 m below the ground surface.

of drying is greater when the depth of freezing is greater. When these data are viewed in the context of snow cover data described in the previous section, it is clear that the depth of freezing is greater when snow cover is thinner.

4.2.5. Shallow pore pressure and velocity variations

Pore pressures within the landslide are probably the most important (and most difficult to obtain) pieces of information that can lead to an understanding of seasonal variations in landslide movement. Under ideal circumstances, pore pressures should be measured at multiple locations at the shear surface(s) at the base of the landslide. Because the active part of the Slumgullion landslide is estimated to be 12–30 m thick (Baum and Reid, 2000), hand augering to the basal shear surface is not possible. Also, the remote and topographically rugged setting of the landslide makes drilling difficult and expensive. As described in Methods, we instrumented one 2.2 m deep, hand-augered well near an intermittent pond at station IS2 to gain a preliminary understanding of pore pressures within the landslide. Hourly pore pressures measured by the piezometer in this hole, as well as landslide velocities and soil temperature at IS2, and daily precipitation at IS1, are shown in Fig. 18.

Landslide velocities corresponded with precipitation throughout the year and seasonally corresponded with shallow pore pressure (Fig. 18). The periods of greatest velocity corresponded with the periods of relatively high pore pressures coincident with spring snowfall and snowmelt. Secondary peaks in velocity corresponded with an increase in pore pressure from summer rainfall. Each passing rainstorm had a rapid (within several weeks) effect on pore pressures and velocities. Minimum velocities corresponded with minimum or near minimum precipitation and pore pressures in early winter. From mid-winter to early spring, however, increases in landslide velocity tended to coincide with snowfall but precede increases in shallow pore-pressure. That is, during each WY, landslide velocities began to increase in mid-winter, as days became longer, air temperatures gradually increased, and snow intermittently melted, whereas pore pressure did not begin to increase until the major spring snowmelt began. We do not understand the reason(s) for this pattern, but present several possible explanations in the following section.

5. Discussion

5.1. Causes for seasonal variability in landslide velocity

Seasonal variations in velocity demonstrate that landslide movement is affected by meteorologic and hydrologic fluctuations. It would seem that pore pressures at the basal shear surface(s) of the landslide control the landslide velocity. Unfortunately, until wells can be drilled that penetrate the basal surface and piezometers can be installed, we can only make inferences about pore pressures at the basal surface.

Currently available data suggest that seasonal changes in movement are most likely related to changing pore pressures that are controlled by the infiltration of surface water. The infiltration of surface water is a function of the availability of water from snowmelt or rainfall and the permeability of the landslide material. Rising and falling pore pressures would respectively decrease or increase the effective normal stress at the basal surface of the landslide. According to the Mohr–Coulomb failure criterion for effective stress (Terzaghi, 1943), a change in effective normal stress results in a corresponding change in resisting shear stress along the base of the landslide. The velocity of the landslide, therefore, increases or decreases in response to increasing or decreasing pore pressures.

Our preliminary interpretation of the first year of data collected during this study (Coe et al., 2000b) primarily focused on the role that frozen ground at and near the landslide surface played in affecting surface water infiltration and subsurface water levels. Previous work at other locations has shown that frozen ground can dramatically decrease surface water infiltration by blocking soil pores with ice (Kane, 1980; Kane and Stein, 1983; Stähli et al., 1999) and that the water content of the soil is the primary factor that controls the degree to which freezing changes infiltration, that is, infiltration rates in frozen ground decrease with increasing water content. The clay-rich Slumgullion landslide has a high soil-water content (30–65%, Fig. 17; Chleborad et al., 1996), suggesting that infiltration rates would be dramatically affected by freezing and thawing. However, the 2.5 years of additional data lead us to suggest that the infiltration of surface water, and thus subsurface water levels and landslide movement, is primarily controlled by the availability of water from

snowmelt or rainfall, and is secondarily affected by the frozen or unfrozen state of the landslide. We make this statement for several reasons. First, changes in landslide velocities generally coincide with changes in precipitation throughout the year regardless of the frozen or unfrozen state of the ground (Fig. 18). Second, on an annual basis, landslide movements at individual points and stations were greatest during the WY 1999 winter when the landslide was frozen at 20 cm for the longest period and mid-winter snowmelt was the greatest (Figs. 11 and 16a). Lastly, although soil moisture data at IS1 indicate that drying occurs below frozen ground (Fig. 17), presumably because the frozen ground blocks the infiltration of surface water, field observations indicate that there are large patches of bouldery debris on the landslide surface and that much of the landslide is being fractured and jumbled by continuous movement throughout the year (Fig. 19). We suspect that the patches of bouldery debris, as well as the fractures and fracture zones, provide conduits through which surface water can infiltrate regardless of the frozen or unfrozen nature of the surrounding landslide matrix material.

As stated in the previous section, we do not understand the observed increase in landslide velocity prior to an increase in shallow pore pressures during each winter and early spring (Fig. 18), although several explanations seem plausible, albeit speculative. Data that we have available seem to suggest that during the period when the landslide is not frozen, the pore pressure response measured in the shallow hole is closely coupled to the inferred pore pressure response at the basal shear surface. However, during the period when the landslide is frozen or nearly frozen, the pore pressure response in the shallow hole seems to be decoupled from the pore pressure response at the basal shear surface. This inferred relationship implies that water in the shallow hole may be perched with respect to the overall (deeper?) ground-water system in the winter, when ground-water levels are relatively low, or that other factors, such as snow load or changing barometric pressures (e.g., Köhler and Schulze, 2000), may be affecting landslide velocity.

Baum and Reid (2000) have used the analogy of a clay-lined bathtub in attempting to explain the persistent movement of large translational landslides in the western United States, including Slumgullion. In this model, the landslide is isolated both mechanically and hydrologically from adjacent materials by low permeability clays. At Slumgullion, the model would suggest that pore pressures at the basal shear surface are always adequate to maintain movement because the low permeability clays cause the landslide to retain water. Our data fit this model as follows. Minimum velocities in early to mid-winter correspond to low ground-water levels and inferred low pore pressures at the basal shear surface. Velocities gradually increase as periodic mid-winter snowmelt infiltrates the landslide surface and presumably causes pore pressures to increase at the basal shear surface. Velocities peak when spring snowmelt rapidly infiltrates to the basal surface and increases pore pressures. Velocities begin to decrease as pore pressures decrease during the early summer dry season (May and June). Velocities increase again when mid-to-late summer rains start. Each passing rainstorm increases pore pressures and thus velocities. Velocities progressively decrease into the fall and winter as temperatures become colder and some precipitation begins to be stored in the form of snow. During January, the coldest (Fig. 16a), and one of the driest times of year at Slumgullion (Fig. 18), water levels and pore pressures reach a low and velocities are at a minimum.

Key elements to the bathtub model are (1) given an adequate source of material, driving force, and meteorologic conditions, pore pressures are always adequate to maintain movement, and (2) any infiltration of water at the surface of the landslide is sufficient to rapidly increase pore pressures and thus landslide velocity. The relatively quick response (within several weeks) of landslide velocities to precipitation events observed at Slumgullion is presumably typical for other large, clay-rich landslides (four landslides in Utah and one in Hawaii) cited by Baum and Reid (2000), and for a large landslide along Highway 50 in California (Reid, 2002; Reid, oral communication, 2002), but not typical for others, such as the Minor Creek landslide in northwestern California, where velocity increases occur several months after precipitation (Iverson and Major, 1987). In order for the model to apply at Slumgullion, the landslide must contain high permeability zones where water can rapidly infiltrate and affect pore pressures at the basal shear surface. We suspect that many of these zones are patches of bouldery debris or fractures. High permeability zones clearly exist at Slumgullion as evidenced by sinks and perennial springs on the landslide (Fleming et al., 1999).

Fig. 19. Photograph of the deformed and jumbled landslide surface northwest of GPS point MP10. View is across the landslide from southeast to northwest. Almost the entire width of the landslide is visible. The width visible from this position is about 150 m. Photograph taken January 5, 2000.

5.2. Causes for annual variability in landslide movement

Annual movements measured by GPS and CETs gradually decreased in each succeeding WY during the monitoring period (Figs. 11 and 15). Maximum annual movement during the WY 1999 seems easy to understand because total precipitation in WY 1999 was the highest on record (at the SNOTEL station), the snow water equivalent was the highest in the monitoring period, the duration of snowmelt was the longest in the monitoring period, and summer rainstorms were especially strong. However, an understanding of why movement during the WY 2000 was greater than movement in WY 2001 is more difficult to explain, mainly because total precipitation and snow water equivalent were greater in WY 2001 than in WY 2000 (Fig. 3). Summer rainfall was similar in both years (Figs. 5 and 18). We do not know the reason for the disparity in movement, although we suspect it may be related to several factors. First, the inferred high ground water levels during WY 1999 may have a multiple year effect on landslide movement. That is, landslide movements in WY 2000 may have been

higher than in WY 2001 because the landslide was still partially responding to ground water that was stored in the landslide during WY 1999. Second, the duration of snowmelt was longer in WY 2000 than in WY 2001 (mid-January to early May in WY 2000, and mid-January to late April in WY 2001). More water may infiltrate the landslide and affect pore pressures during a long snowmelt season than during a short snowmelt season when a larger percentage of water may run off in surface streams.

Another possible explanation for the apparent disparity between annual movement and annual precipitation is that the somewhat arbitrary water-year cycle (October 1 to September 30) is out of phase with the annual cycle of landslide movement and precipitation at Slumgullion. The annual cycle of landslide velocity, for example, reaches a minimum about mid-January of each year (Figs. 16a and 18). The timing of this minimum corresponds to a period of time when precipitation and air temperatures are also low (Figs. 16a and 18). Therefore, a more reasonable annual cycle at Slumgullion may be from mid-January to mid-January (January 15 to January 14). When movement data are compiled on the basis of this cycle (Fig. 20), which we refer to as a movement year (MY, e.g. MY 1999 is from January 15, 1999 to January 14, 2000), they show a similar pattern to data compiled on the basis of WYs (Fig. 11), that is, in general, both data sets show a progressive decrease in movement in each successive year. However, when annual precipitation data are compiled on the basis of MYs (Fig. 20), each progressive MY shows a decrease in precipitation, which does not match annual precipitation compiled on the basis of WYs (Fig. 3), but does correspond with the progressive decrease in annual movement that was observed for WYs and MYs (Figs. 11 and 20). This correspondence suggests that MYs may be more appropriate than WYs for compilations of annual data at Slumgullion.

5.3. Differences in the timing of maximum velocities

In WY 2000 and WY 2001, maximum velocities occurred at the same time on different parts of the landslide. In WY 1999, however, maximum velocities occurred at different times on different parts of the landslide (Fig. 12). The disparity in timing of maximum velocities in WY 1999, and not in the other WYs, may have been caused by the record level of precipitation that fell in WY 1999 (Fig. 3). In WY 1999, maximum velocities on the upper and middle parts of the landslide (GPS points MP1–MP15 with elevations above about 3040 m) occurred between May 12 and July 28. On the lower part of the landslide (GPS points MP16–MP19 at elevations below about 3040 m), maximum velocities occurred between March 24 and May 12. The 3040 m elevation coincides approximately with the location of a large pond (Fig. 7A) that may have been created when the toe of the active landslide emerged from, and overrode old landslide deposits (see Parise and Guzzi, 1992; Fleming et al., 1999; and discussion below). The disparity in timing of maximum velocities suggests that different parts of the landslide are acting somewhat independently from one another. Similar observations have been reported for the Aspen Grove landslide in Utah (Baum et al., 1993) and for the Acquara–Vadoncello landslide in Italy (Wasowski and Mazzeo, 1998).

The difference in timing of maximum velocities is probably caused by warmer temperatures at the toe of the landslide than at the middle and upper parts. There is a 500 m difference in elevation between the lowest and highest parts of the landslide. Adiabatic temperature lapse rates (9.8 and 5 °C per thousand meters of elevation for dry and wet air, respectively, from Barry, 1992) suggest that air temperatures for the lowest part of the landslide are 2.5–4.9 °C warmer than those at the upper part of the landslide. Air temperature data from station IS1 (elevation 3180 m) and the SNOTEL station (elevation 3487 m) support this inference. We subtracted the average daily temperature at the SNOTEL station (Fig. 5) from the average daily temperature at station IS1 and found that the difference averaged 2.5 °C (about +1 °C for every 123 m decrease in elevation). This difference indicates that the average difference in air temperature between the head and toe of the active landslide would be about 4 °C. This difference in temperature would cause ground on the lower part of the landslide to remain unfrozen for longer periods of time than that at higher elevations. Additionally, snow would melt earlier and faster on the lower part of the landslide as compared to the upper part. Furthermore, observations of snow depth made during winter GPS surveys indicate that less snow falls on the lower part of the landslide than

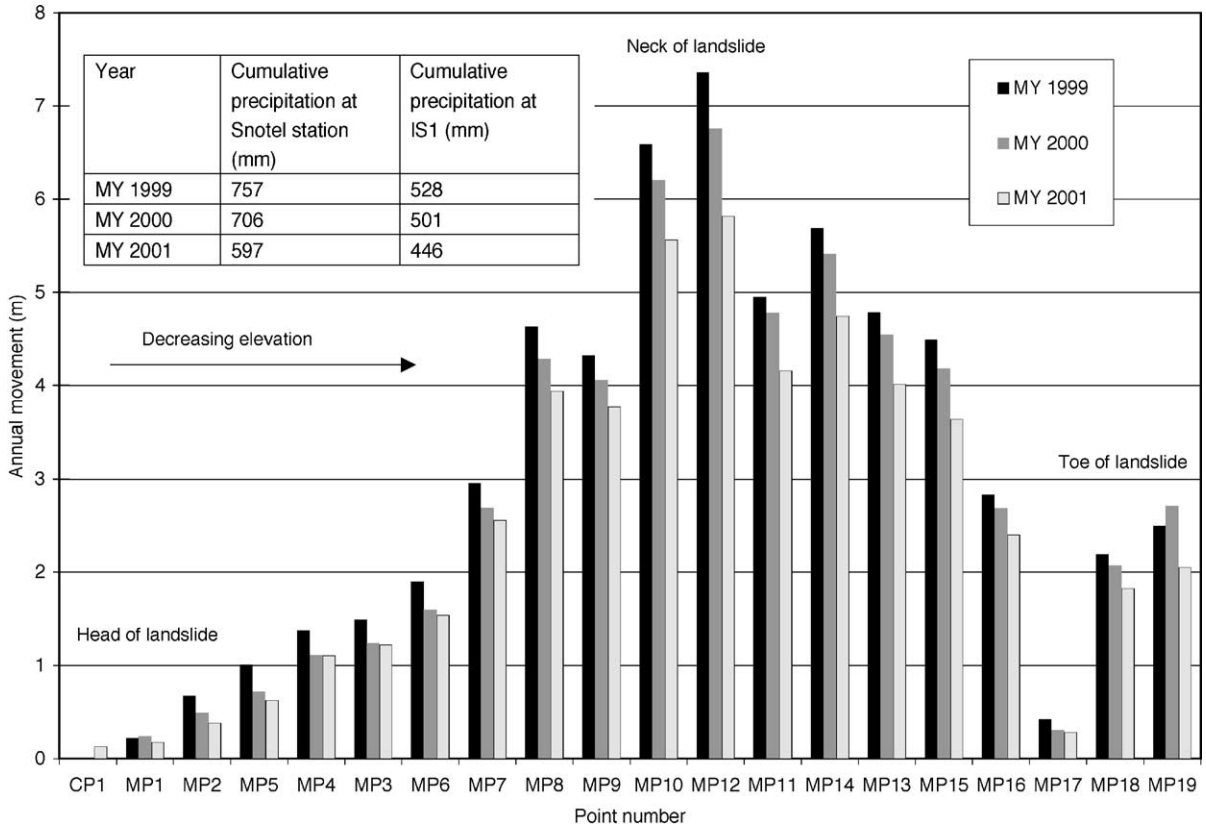

Fig. 20. Bar graph showing the annual horizontal movement of GPS monitoring points in each movement year (MY). Location of monitoring points shown in Fig. 2b. Annual movement at IS2 shows the same pattern. The annual movement at IS2 for each MY is 2.52, 2.28, and 2.10 m, for MY 1999, MY 2000, and MY 2001, respectively. Inset table shows cumulative precipitation during each MY.

on the upper and middle parts. Less snow and more rapid snowmelt suggest that the period of spring surface-water infiltration would be earlier and shorter on the lower part of the landslide than on the upper and middle parts. The difference in the amount of snowfall and the rate of snowmelt on the upper and lower parts of the landslide is readily visible in spring months. Thawing and melting of frozen ground and snow on the lower part of the landslide in the spring probably raises the ground-water level within the landslide, which increases the landslide velocity. In the summer of WY 1999, when ground-water levels and velocities were decreasing on the lower part of the landslide, they were peaking on the upper and middle parts of the landslide when snowmelt there was at a maximum. These observations are supported by work by Chleborad (1998) that identifies a correspondence between the timing of snowmelt-triggered landslides and air temperature.

5.4. Variable velocity response to seasonal changes

The upper part of the landslide responds more dramatically to seasonal changes than the middle and lower parts. Maximum velocities of points on the upper part of the landslide are up to 33 times greater than minimum velocities, whereas for most of the lower and middle parts of the landslide, maximum velocities are about 1.6 times greater than minimum velocities (Fig. 13). The dramatic change along the upper part of the landslide could be caused by several factors. First, because of the colder air temperatures at the head of the landslide, precipitation falls in the form of snow for a longer period of time than at lower elevations. Once

on the ground, the snow also takes longer to melt than at lower elevations. This situation dramatically reduces the amount of water available for infiltration into the upper part of the landslide. Thus, ground-water levels are probably more dramatically reduced, for longer periods of time, as compared to the middle and lower parts of the landslide. Second, because there is more snow available on the upper part of the landslide, the melting of this snow in the spring and summer would provide a greater influx of surface water than that received by lower elevations, thus ground water levels are probably increased more dramatically than on the middle and lower parts of the landslide. Lastly, because the upper part of the landslide is undergoing extension, and the lower part is undergoing longitudinal shortening, the upper part may have more open fractures to receive surface water than the lower part.

5.5. Relation between landslide structures and velocities

Velocities vary gradually along the length of the landslide, with the lowest velocities occurring at points near the head and toe, and highest velocities occurring in the neck. This velocity distribution (Fig. 10) is consistent with patterns established by earlier photogrammetric studies (Powers and Chiarle, 1996; Smith, 1996). The velocity distribution appears to be largely a function of the hourglass-shaped lateral boundaries of the landslide (Fleming et al., 1996; also observed at the Aspen Grove landslide in Utah by Baum et al., 1993). Locally, however, velocities deviate from this distribution according to the location of major structural elements. This is especially evident at points located in pull-apart basins and on opposite sides of southwest–northeast trending strike-slip faults (see Fig. 2b). Velocities of points MP11 and MP17, for example, are anomalously low when compared to surrounding points (Fig. 10). MP11 is located in a pull-apart basin along the north flank where the landslide widens (described by Baum and Fleming, 1996; Fleming et al., 1999) and MP17 is located on the northwest moving side (Fig. 2b) of a strike-slip fault along the north flank of the toe. Velocities of MP13 and MP14, which are about 150 m apart (Fig. 2b), but on opposite sides of a large strike-slip fault, are significantly different, with MP14 on the southern side moving about 20% faster than MP13 on the northern side (first observed by Fleming et al., 1999). These observations indicate that different parts of the landslide are acting somewhat independently from one another (as also indicated by differences in timing of maximum velocities).

5.6. Movement of CP1 and MP1

Movement of CP1 and MP1 was somewhat unexpected because the points are in areas near the head of the landslide that were previously mapped as inactive (Figs. 1, 2, and 21). Point CP1 is on what appears to be deeply weathered, highly altered bedrock. During the 3.5-year monitoring period, CP1 moved about 0.54 m to the west (azimuth = 279°) at an average velocity of about 0.03 cm/day. Point MP1 is on a ridge that parallels and is upslope from the active flank ridge (Fig. 21). During the monitoring period, MP1 moved 0.75 m to the southwest (azimuth = 245°) at an average horizontal velocity of 0.06 cm/day. These movements and velocities are low compared to the main body of the landslide. MP2 (Fig. 21), for example, moved 1.87 m to the southwest (azimuth = 224°) at an average velocity of 0.14 cm/day during the monitoring period. The higher velocity of the main body of the landslide evidently allows the flank ridge bordering the main landslide (Fig. 21) to remain intact.

5.7. Movement of MP16

Point MP16, located on pond sediments just southwest of an intermittent pond on the lower part of the landslide (Fig. 22), is moving upward in elevation (see Coe et al., 2000a). All other monitoring points are moving downward in elevation. The point increased 0.59 m in elevation between July 1998 and March 2002. Previous studies (Parise and Guzzi, 1992; Fleming et al., 1999) have suggested that the location of the pond is controlled by a depression at the basal surface of the landslide, which was created when the toe of the active landslide emerged and overrode old landslide deposits. By emerging from, and overriding existing deposits, debris in the active landslide was backtilted, forming a closed depression that pools water. These studies also suggested that the pond location remains fixed over time while landslide debris is transported into the pond, receives a coating of pond sediments, and is then transported out of the pond. The upward movement of MP16 and a backtilted trail of pond

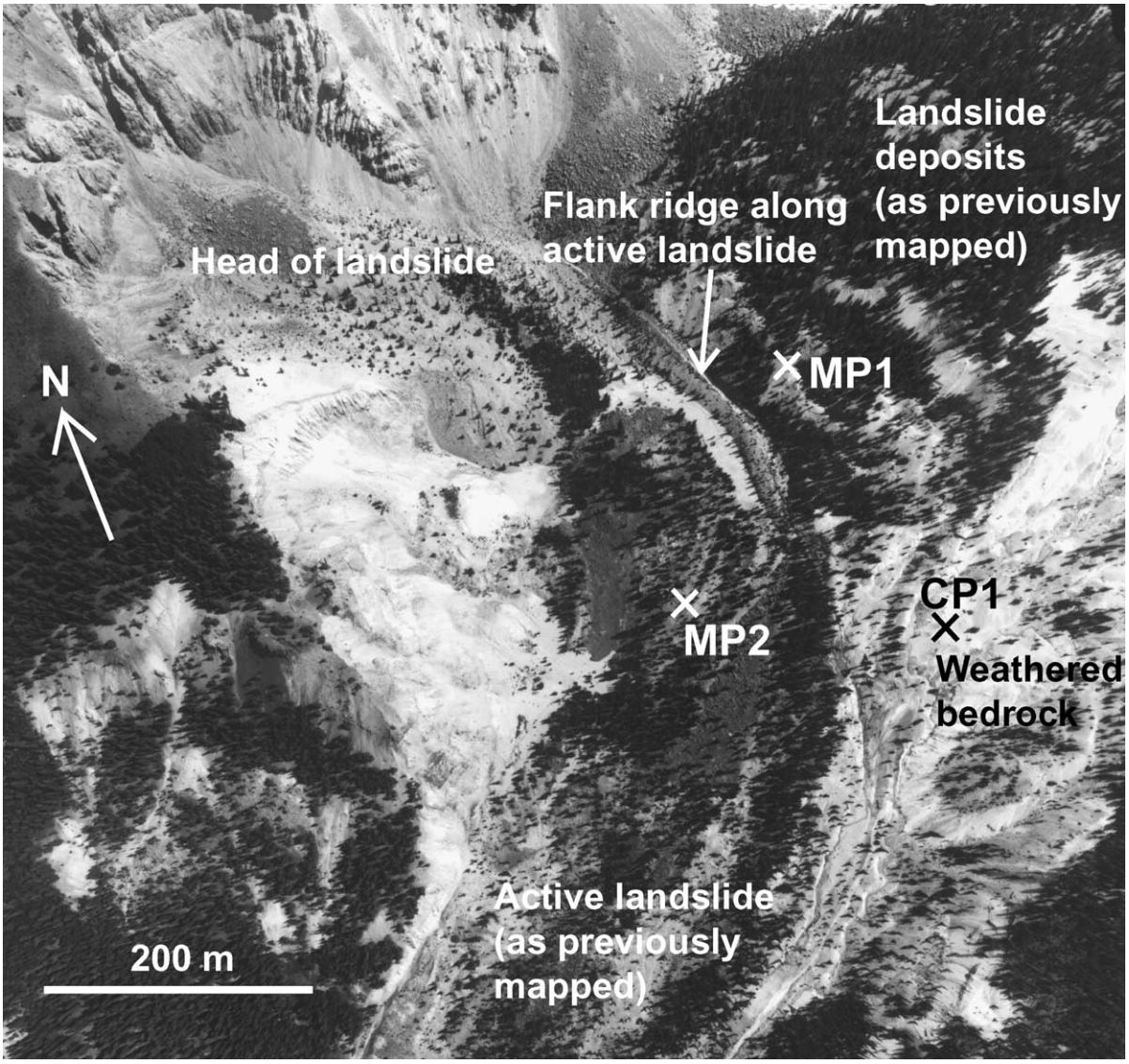

Fig. 21. Aerial photograph of the upper part of the landslide showing the locations of GPS points MP1, MP2, and CP1. USGS aerial photograph number 3B-1 taken July 31, 2000.

sediments southwest of the pond (Fig. 22) supports this hypothesis.

5.8. Comparison of annual movements to previously measured movements

A comparison of annual rates of movement measured in this study to movements reported in previous studies (Fig. 23) reveals that, in general, movements measured in WY 1999, WY 2000, and WY 2001 were greater than previous years at points downslope from MP6 (MP7–MP16, MP18, MP19, Fig. 2b), and less than previous years at points upslope from MP6 (MP2–MP6, Fig. 2b). Movements were not previously measured at CP1 and MP1. For this comparison, we compiled our data on the basis of WYs, rather than MYs, because many of the previous data were based on measurements made during summer months and

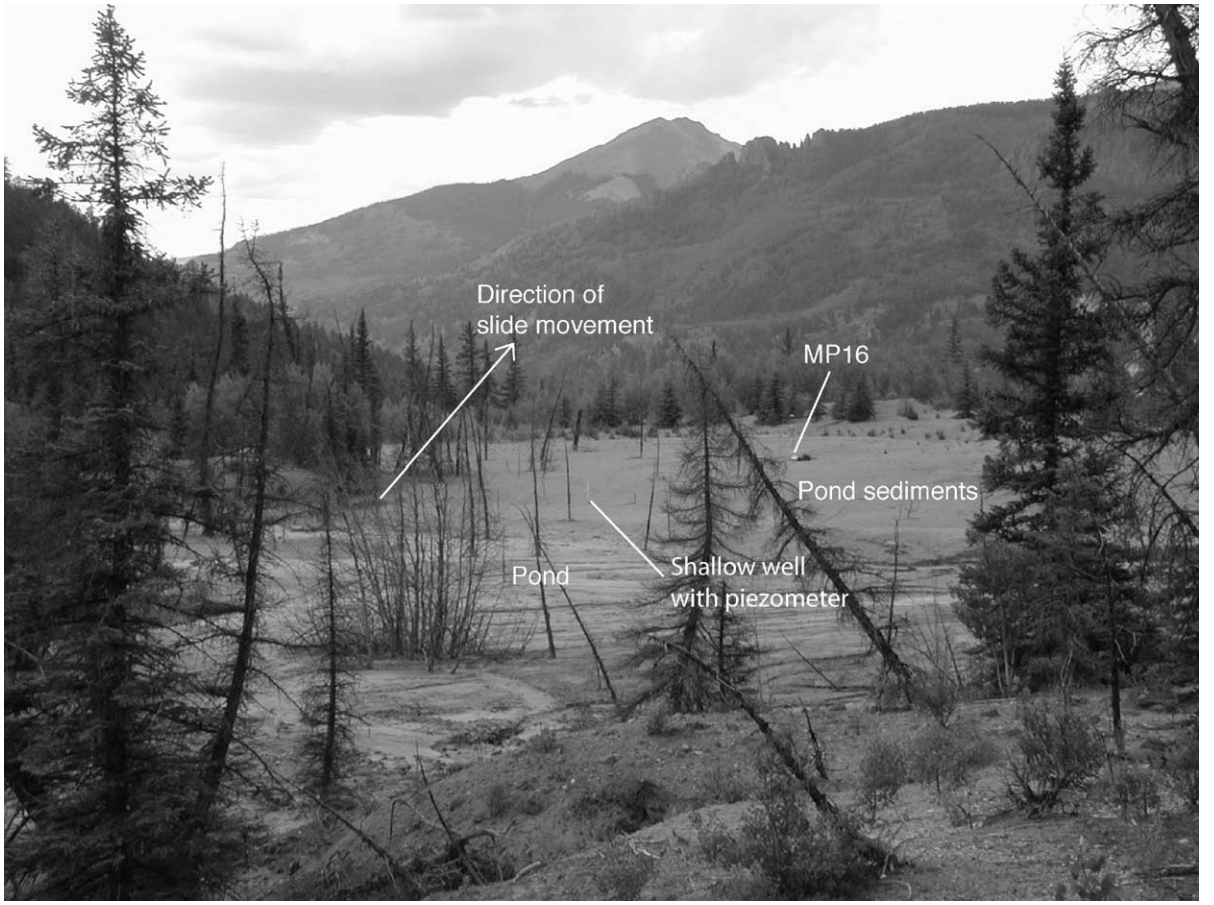

Fig. 22. GPS monitoring point MP16 looking downslope. Backtilted pond sediments surround MP16. The width of the pond visible from left to right is about 60 m. The shallow well with piezometer (recorded at station IS2) is also visible in the field of view. View is to the south. Photo taken July 20, 2001.

therefore more closely correspond to the WY time frame (October 1 to September 30).

The reasons for the differences in annual movements are unclear, although several explanations seem plausible. First, at least some of the differences are due to inherent differences in measurement techniques. Annual velocities in most previous studies were determined by averaging movement measured from photo identifiable features in aerial photographs taken in 1985 and 1990. We used movement maps generated by these studies to estimate movements at our point positions. Movements in this study were measured about every 69 days and interpolated to match the beginning and ending of individual WYs. Second, some of the differences are real and are probably caused by variation in amounts and timing of precipitation. The WY 1999, for example, was clearly an exceptional year for landslide movement, probably because it was the wettest year on record (at the SNOTEL station). Additionally, annual movements between 1985 and 1990 were relatively low, probably because many of these years had some of the lowest precipitation on record (at the SNOTEL station, Fig. 3).

The disparity in movement history of points on the upper part of the landslide versus those on the middle and lower parts of the landslide is also not easily explained. One possible explanation is that the upper part of the landslide is gradually slowing because the volume of material at the head of the landslide no longer provides an adequate driving force to maintain

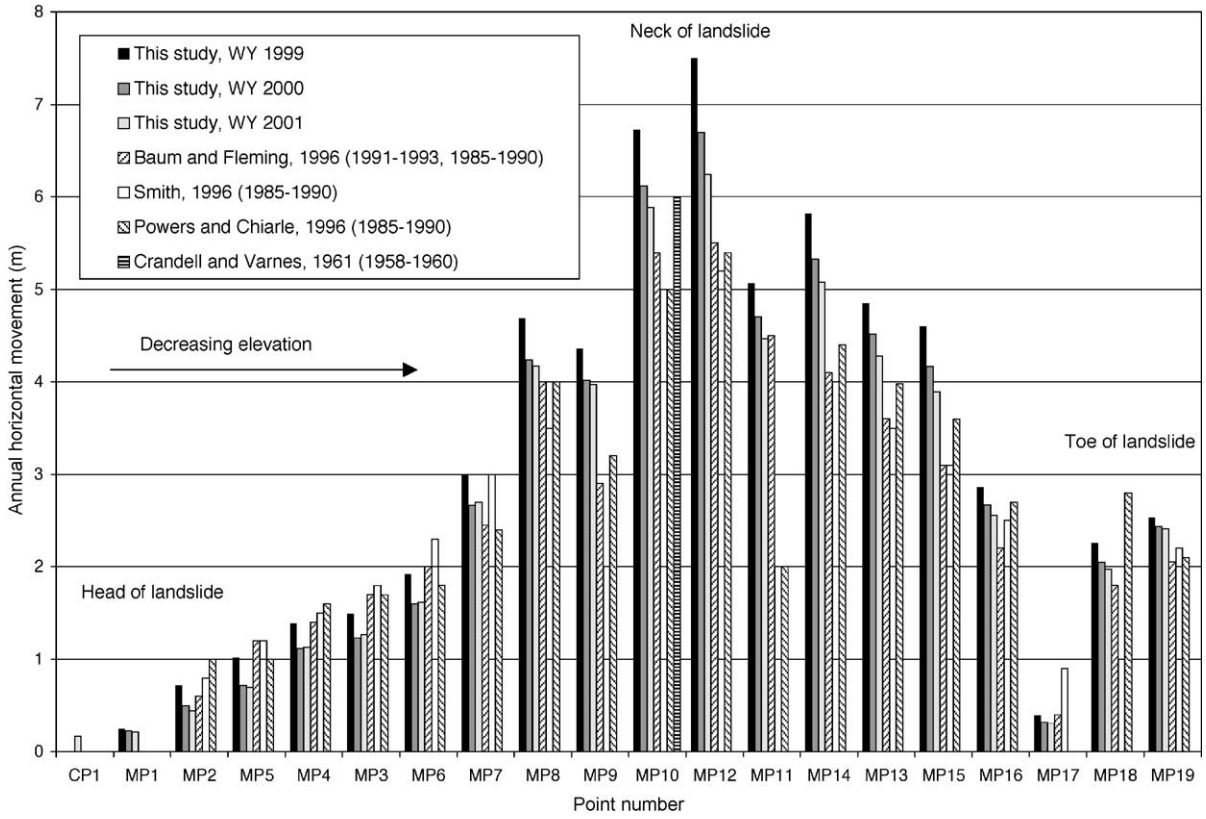

Fig. 23. Bar graph showing annual horizontal movement of individual points from this study compared to previous measurements.

movements documented in the past. At least one piece of geomorphic evidence, the decreasing height and lateral extent of landslide bounding flank ridges along the upper and middle parts of the landslide, support this explanation (Fleming et al., 1999). Continued monitoring should help to clarify the causes of variability in annual movement.

6. Conclusions

Data from GPS surveys and field instrumentation lead us to make the following conclusions regarding movement of the Slumgullion landslide.

(1) Landslide movement was continuous throughout the 3.5-year monitoring period but velocity varied on a seasonal basis. Landslide velocity increased in response to snowmelt and rainfall and decreased during dry periods. The time between rainfall and the landslide velocity and shallow pore pressure response was less than several weeks. The lowest velocities occurred in mid-winter when air temperatures were at or near yearly minimums, the near-surface landslide material was frozen, and water was stored on the landslide surface as snow. We suggest that variability in velocities is primarily controlled by the availability of surface water from melting snow or rainfall, and that surface water quickly infiltrates the landslide through patches of bouldery debris or fractures that are created by continuous movement. We also suggest that the continuous but seasonally variable landslide movement observed at Slumgullion fits the bathtub model for landslide movement described by Baum and Reid (2000).

(2) On an annual basis, landslide movements were greatest during WY 1999 (October 1, 1998 to September 30, 1999) and progressively decreased in each succeeding water year. Compared to the succeeding water

years, WY 1999 had the highest total precipitation, longest duration of snowmelt, and highest precipitation from summer thunderstorms. Also, unlike succeeding water years, maximum spring velocities in WY 1999 occurred at different times on different parts of the landslide. On the lower part of the landslide, maximum velocities occurred between March 24 and May 12, whereas on the middle and upper parts of the landslide, maximum velocities occurred between May 12 and July 28. This discrepancy was probably caused by frequent, wintertime melting of anomalously high snowfall (compared to succeeding winters) and by warmer air temperatures at the lower part of the landslide (about 4 °C) that triggered the melting of snow earlier than at the upper and middle parts of the landslide.

(3) During all WYs monitored, annual movements and average daily velocities were smallest at the head and toe of the landslide and largest in the central, narrowest part of the landslide. Movements and velocities deviated from this distribution in areas where they were affected by major structural elements within the landslide. In general, annual movements measured on the lower and middle parts of the landslide were greater than any previously documented, whereas annual movements measured on the upper part of the landslide were less than previously documented. This implies that the driving force responsible for moving the upper part of the landslide may be less than it has been in the past.

(4) Movement was measured on landslide deposits near the head of the landslide that were previously identified as inactive. This observation indicates that the active landslide is larger and more complex than previously recognized.

Acknowledgements

We dedicate this paper to David Varnes, our friend and colleague who passed away in February 2002. Dave's research at Slumgullion spanned more than 40 years and provided guidance and inspiration for those of us who have followed. We thank Bob Fleming and Mark Reid for suggestions that helped focus this study. We are grateful to Perry Hardin, Nicolas Houdré, Caroline Arnal, Manuelle Seigneur, Graham MacDonald, Oswaldo Filho, David Varnes, Kathy Varnes, Josh Ellis, Pierre Tachker, Edouard Mine, Erica Bigio, Jon McKenna, and John McDowell for their assistance with GPS surveys at various times. Mark Reid and Rex Baum provided guidance and assistance with the initial installation of field instruments and had helpful suggestions throughout the study. Rex Baum also programmed the Campbell data loggers. We thank Bob Fleming, Al Chleborad, Janusz Wasowski, Vern Singhroy, Rex Baum, and Vincenzo del Gaudio for their critical reviews of this paper. Karen and Dave Mourhess and David and Candy Beebe were gracious hosts during our stays at the Matterhorn Mountain Lodge in Lake City. This study was funded by the NASA Solid Earth and Natural Hazards research program (NRA-MTPE-1997-10), Principal Investigators, David Arnold and David Long, Brigham Young University, and Co-Investigator, Jeff Coe, USGS.

References

Atwood, W.W., Mather, K.F., 1932. Physiography and Quaternary geology of the San Juan mountains, Colorado. U.S. Geological Survey Professional Paper 166, 163–164.

Avery, B.A., Jones, C.N., Colton, J.D., Meyers, M.P., 2001. A southwest Colorado mountain flash flood in an enhanced monsoonal environment. Unpublished National Weather Service Report, Grand Junction, Colorado. http://www.crh.noaa.gov/gjt/papers/flashflood/flashflood.htm.

Barlow, M., Nigam, S., Berbery, E.H., 1998. Evolution of the North American monsoon system. Journal of Climate 11, 2238–2257.

Barry, R.G., 1992. Mountain Weather and Climate, 2nd ed. Routledge, London, 402 pp.

Baum, R.L., Fleming, R.W., 1996. Kinematic studies of the Slumgullion landslide, Hinsdale County, Colorado. In: Varnes, D.J., Savage, W.Z. (Eds.), The Slumgullion Earth Flow: A Large-Scale Natural Laboratory. U.S. Geological Survey Bulletin, vol. 2130, pp. 9–12.

Baum, R.L., Reid, M.E., 2000. Ground water isolation by low-permeability clays in landslide shear zones. In: Bromhead, E.N., Dixon, N., Ibsen, M.-L. (Eds.), Landslides in Research, Theory and Practice. Proc. 8th Int. Symp. on Landslides, Cardiff, Wales, vol. 1. Telford, London, pp. 139–144.

Baum, R.L., Fleming, R.W., Johnson, A.M., 1993. Kinematics of the Aspen Grove landslide, Ephraim Canyon, central Utah. U.S. Geological Survey Bulletin 1842-F, 4–12.

Chleborad, A.F., 1998. Use of air temperature data to anticipate the onset of snowmelt-season landslides. U.S. Geological Survey Open-File Report 98-124, 16 pp.

Chleborad, A.F., Diehl, S.F., Cannon, S.H., 1996. Geotechnical properties of selected materials from the Slumgullion landslide. In: Varnes, D.J., Savage, W.Z. (Eds.), The Slumgullion Earth Flow: A Large-Scale Natural Laboratory. U.S. Geological Survey Bulletin, vol. 2130, pp. 67–71.

Coe, J.A., Godt, J., Chleborad, A., Harp, E., Savage, W.Z., Tachker P., 1999. Debris flows triggered by the rainstorm of July 28, 1999, Interstate-70 corridor, Georgetown to the Eisenhower Tunnel, central Colorado. Unpublished U.S. Geological Survey report (http://www.lanslides.usgs.gov/i70/).

Coe, J.A., Godt, J.W., Ellis, W.L., Savage, W.Z., Savage, J.E., Powers, P.S., Varnes, D.J., Tachker, P., 2000a. Seasonal movement of the Slumgullion landslide as determined by GPS observations, July 1998–July 1999. U.S. Geological Survey Open-File Report 00-101, 47 pp. (http://www.greenwood.cr.usgs.gov/pub/open-file-reports/ofr-00-0101/).

Coe, J.A., Godt, J.W., Ellis, W.L., Savage, W.Z., Savage, J.E., Powers, P.S., Varnes, D.J., Tachker, P., 2000b. Preliminary interpretation of seasonal movement of the Slumgullion landslide as determined by GPS observations, July 1998–July 1999. U.S. Geological Survey Open-File Report 00-102, 25 pp. (http://www.greenwood.cr.usgs.gov/pub/open-file-reports/ofr-00-0102/).

Colorado Geological Survey, 1999. ROCKTALK 2 (4), 1–4.

Crandell, D.R., Varnes, D.J., 1961. Movement of the Slumgullion earthflow near Lake City, Colorado. Short Papers in the Geologic and Hydrologic Sciences. U.S. Geological Survey Professional Paper 424-B, 136–139.

Diehl, S.F., Schuster, R.L., 1996. Preliminary geologic map and alteration mineralogy of the main scarp of the Slumgullion landslide. In: Varnes, D.J., Savage, W.Z. (Eds.), The Slumgullion Earth Flow: A Large-Scale Natural Laboratory. U.S. Geological Survey Bulletin, vol. 2130, pp. 13–19.

Eldredge, E.P., Shock, C.C., Steiber, T.D., 1993. Calibration of granular matrix sensors for irrigation management. Agronomy Journal 85 (6), 1228–1232.

Endlich, F.M., 1876. Report of F.M. Endlich. In: U.S. Geological and Geographical Survey (Hayden) of the Territories Annual Report 1874, 203 pp.

Fleming, R.W., Baum, R.L., Savage, W.Z., 1996. The Slumgullion landslide, Hinsdale County, Colorado. In: Thompson, R.A., Hudson, M.R., Pillmore, C.L. (Eds.), Geologic Excursions to the Rocky Mountains and Beyond. Geological Society of America Special Publication 44, Annual Meeting, 4–6.

Fleming, R.W., Baum, R.L., Giardino, M., 1999. Map and description of the active part of the Slumgullion Landslide, Hinsdale County, Colorado. U.S. Geological Survey Miscellaneous Investigation Series Map I-2672.

Gili, J.A., Corominas, J., Rius, J., 2000. Using Global Positioning System techniques in landslide monitoring. Engineering Geology 55, 167–192.

Gomberg, J., Bodin, P., Savage, W.Z., Jackson, M.E., 1995. Landslide faults and tectonic faults, analogs: the Slumgullion earthflow, Colorado. Geology 23 (1), 41–44.

Hales Jr., J.E. 1974. Southwest United States summer monsoon source—Gulf of Mexico or Pacific Ocean? Journal of Applied Meteorology 13, 331–342.

Hansen, E.M., 1975. Moisture source for three extreme local rainfalls in the southern Intermountain region. National Oceanic and Atmospheric Administration Technical Memorandum NWS Hydro-26, 57 pp.

Iverson, R.M., Major, J.J., 1987. Rainfall, ground-water flow, and seasonal movement at Minor Creek landslide, northwestern California—physical interpretation of empirical relations. Geological Society of America Bulletin 99, 579–594.

Jackson, M.E., Bodin, P.W., Savage, W.Z., Nel, E.M., 1996. Measurement of local velocities on the Slumgullion landslide using the Global Positioning System. In: Varnes, D.J., Savage, W.Z. (Eds.), The Slumgullion Earth Flow: A Large-Scale Natural Laboratory. U.S. Geological Survey Bulletin, vol. 2130, pp. 93–95.

Kane, D.L., 1980. Snowmelt infiltration into seasonally frozen soils. Cold Regions Science and Technology 3, 153–161.

Kane, D.L., Stein, J., 1983. Water movement into seasonally frozen soils. Water Resources Research 19 (6), 1547–1557.

Köhler, H.-J., Schulze, R., 2000. Landslides triggered in clayey soils—geotechnical measurements and calculations. In: Bromhead, E., Dixon, N., Ibsen, M.-L. (Eds.), Landslides in Research, Theory, and Practice. Proc. 8th Int. Symp. on Landslides, Cardiff, Wales, vol. 2. Thomas Telford, London, pp. 837–842.

Leick, A., 1990. GPS Satellite Surveying Wiley, New York, 352 pp.

Lipman, P.W., 1976. Geologic map of the Lake City caldera area, western San Juan Mountains, southwestern Colorado. U.S. Geological Survey Miscellaneous Investigation Series Map I-962.

Löve, D., 1970. Subartic and subalpine—where and what? Artic and Alpine Research 2, 63–72.

Madole, R.F., 1996. Preliminary chronology of the Slumgullion landslide, Hinsdale County, Colorado. In: Varnes, D.J., Savage, W.Z. (Eds.), The Slumgullion Earth Flow: A Large-Scale Natural Laboratory. U.S. Geological Survey Bulletin, vol. 2130, pp. 5–7.

Malet, J.P., Maquaire, O., Calais, E., 2002. The use of Global Positioning System techniques for the continuous monitoring of landslides—application to the Super-Sauze earthflow (Alpes-de Haute-Provence, France). Geomorphology 43, 33–54.

Parise, M., Guzzi, R., 1992. Volume and shape of the active and inactive parts of the Slumgullion landslide, Hinsdale County, Colorado. U.S. Geological Survey Open-File Report 92-216, 29 pp.

Powers, P.S., Chiarle, M., 1996. A digital photogrammetric method to measure horizontal surficial movements on the Slumgullion landslide, Hinsdale County, Colorado. In: Varnes, D.J., Savage, W.Z. (Eds.), The Slumgullion Earth Flow: A Large-Scale Natural Laboratory. U.S. Geological Survey Bulletin, vol. 2130, pp. 51–55.

Reid, M.R., 2002. Real-time monitoring of an active landslide above Highway 50, California, unpublished USGS data available on the web (http://www.vulcan.wr.usgs.gov/Projects/CalifLandslide/framework.html).

Savage, W.Z., Fleming, R.W., 1996. Slumgullion landslide fault creep studies. In: Varnes, D.J., Savage, W.Z. (Eds.), The Slumgullion Earth Flow: A Large-Scale Natural Laboratory. U.S. Geological Survey Bulletin, vol. 2130, pp. 73–76.

Sharp, W.N., Martin, R.A., Lane, M.E., 1983. Mineral resource potential of the Powderhorn Wilderness Study Area and Cannibal Plateau Roadless Area, Gunnison and Hinsdale Counties, Colorado. U.S. Geological Survey Miscellaneous Field Studies Map MF-1483-A.

Smith, W.K., 1996. Photogrammetric determination of slope movements on the Slumgullion landslide. In: Varnes, D.J., Savage,

W.Z. (Eds.), The Slumgullion Earth Flow: A Large-Scale Natural Laboratory. U.S. Geological Survey Bulletin, vol. 2130, pp. 57–60.

Stähli, M., Jansson, P., Lundin, L., 1999. Soil moisture redistribution and infiltration in frozen sandy soils. Water Resources Research 35 (1), 95–103.

Terzaghi, K., 1943. Theoretical Soil Mechanics. Wiley, New York 510 pp.

Van Sickle, J., 1996. GPS for Land Surveyors. Ann Arbor Press, Chelsea, MI, 209 pp.

Varnes, D.J., Savage, W.Z., 1996a. Introduction. In: Varnes, D.J., Savage, W.Z. (Eds.), The Slumgullion Earth Flow: A Large-Scale Natural Laboratory. U.S. Geological Survey Bulletin, vol. 2130, pp. 1–4.

Varnes, D.J., Savage, W.Z., 1996b. The Slumgullion earth flow: a large-scale natural laboratory. U.S. Geological Survey Bulletin 2130, 1–4.

Varnes, D.J., Smith, W.K., Savage, W.Z., Powers, P.S., 1996. Deformation and control surveys, Slumgullion landslide. In: Varnes, D.J., Savage, W.Z. (Eds.), The Slumgullion Earth Flow: A Large-Scale Natural Laboratory. U.S. Geological Survey Bulletin, vol. 2130, pp. 43–49.

Wasowski, J., Mazzeo, D., 1998. Some results of topographic monitoring of the Acquara-Vadoncello landslide, Italy. In: Moore, D., Hungr, O. (Eds.), Proc. 8th Int. Congress, International Association for Engineering Geology and the Environment, Vancouver, Canada, vol. 3. Balkema, Rotterdam, pp. 1705–1712.